# BCS-BEC crossover in a system of microcavity polaritons

Jonathan Keeling,* P. R. Eastham, M. H. Szymanska, and P. B. Littlewood
*Cavendish Laboratory, Madingley Road, Cambridge CB3 OHE, U.K.*
(Received 21 February 2005; published 19 September 2005)

We investigate the thermodynamics and signatures of a polariton condensate over a range of densities, using a model of microcavity polaritons with internal structure. We determine a phase diagram for this system including fluctuation corrections to the mean-field theory. At low densities the condensation temperature $T_c$ behaves like that for point bosons. At higher densities, when $T_c$ approaches the Rabi splitting, $T_c$ deviates from the form for point bosons, and instead approaches the result of a BCS-like mean-field theory. This crossover occurs at densities much less than the Mott density. We show that current experiments are in a density range where the phase boundary is described by the BCS-like mean-field boundary. We investigate the influence of inhomogeneous broadening and detuning of excitons on the phase diagram.

DOI: 10.1103/PhysRevB.72.115320 PACS number(s): 71.36.+c, 42.55.Sa, 03.75.Kk

## I. INTRODUCTION

There have been many recent experiments with the aim of observing Bose condensation of polaritons in two-dimensional microcavities. Recent experimental progress includes nonlinear increase of the occupation of the ground state,[1,2] subthermal second-order coherence,[2] changes to the angular dispersion of polariton luminescence,[3–5] increased population of low momentum polaritons,[3] and stimulated processes in resonantly pumped cavities.[6–10] Such experiments, however, do not provide unambiguous evidence for the observation of a polariton condensate as distinct from, e.g., a kind of laser. Theoretical predictions of the detailed properties of polariton condensation are therefore of considerable interest. In this paper, we consider the form of the phase boundary, and experimental signatures of condensation. We include the internal structure of polaritons, and Fermionic structure of excitons.

The phase boundary at low densities may be described by a model of weakly interacting bosons.[11–13] At higher densities, when $T_c$ approaches the Rabi splitting, the phase boundary approaches the result of a BCS-like mean-field theory. Such an interaction dominated mean-field phase boundary requires a model with internal polariton structure. For a zero-dimensional cavity, the mean-field theory is correct at all densities, but in a two-dimensional cavity, fluctuations cause a crossover to the weakly interacting boson limit at low densities. The crossover scale is set by the wavelength of light, rather than average exciton separation, and so occurs at densities much less than the Mott density. The form of the phase boundary changes when the exciton is detuned below the photon. As in the mean-field case,[14] detuning can lead to a multivalued phase boundary. However, with fluctuations this multivalued structure occurs for smaller detunings than are required for the mean-field case.

We also discuss a number of experimentally testable signatures of a coherent state of polaritons. These include dramatic changes in the luminescence and absorption spectra, and in the angular distribution of radiation emitted from the condensate. These signatures are a consequence of a coherent photon field, and of the presence of the Goldstone mode associated with symmetry breaking. In a previous publication,[15] some of these results were presented in the absence of exciton-photon detuning. In this paper we present in full the calculation which led to those results, and extend our results to include detuning and inhomogeneous broadening of the excitons.

We consider a model of localized excitons coupled to a continuum of radiation modes confined in a two-dimensional microcavity. This provides an extension of previous studies[14,16] of the mean-field (zero-dimensional) system. A model of localized excitons is motivated by systems such as organic semiconductors,[17,18] quantum dots,[19–21] and disordered quantum wells.[22] In addition, the predictions of such a model are expected to be similar to those for a model of mobile excitons, since a typical exciton mass is several orders of magnitude larger than the typical photon mass.

We study the behavior of this model in thermal equilibrium. Although current experiments may remain far from equilibrium, there are several reasons to study the equilibrium behavior. As the quality of microcavity fabrication, and in particular the quality, of mirrors improve,[23,24] experiments can be expected to reach states closer to thermal equilibrium. Further, the nature of experimental signatures for coherence close to equilibrium are expected to be similar to those in thermal equilibrium. Finally, the equilibrium distribution may be considered a limiting case of the nonequilibrium problem, when pumping and decay rates are taken to zero, so the equilibrium case is thus instructive in approaching the nonequilibrium problem.

The Hamiltonian we study is similar to the Holland-Timmermans Hamiltonian[25,26] studied in the context of Feshbach resonances in atomic gases. However, there are a number of important differences between the two models; most notably the absence of a direct four-fermion interaction, and the bare fermion density of states. How these differences affect the mean-field results is discussed in Sec. III C, and their effect on the fluctuation spectrum in Secs. III D and III E. Because our system is two dimensional, it is necessary to study fluctuations in the presence of a condensate. Such fluctuations have also been studied recently by Ohashi and Griffin[27] in the context of the Feshbach resonances. However as discussed in Sec. IV A, we disagree with part of their method.

 

The rest of this paper is organized as follows. In Sec. II we introduce the Hamiltonian for our model, and discuss how it will be treated. Section III reproduces the mean-field results presented elsewhere, and then discusses the effective action, and resulting spectrum of fluctuations about it. From the fluctuation spectrum, a number of experimental signatures are also discussed.

In Sec. IV we explain how to calculate fluctuation corrections to the mean-field phase diagram. Some of the issues in this section are associated with the specific details of our model, or with fluctuations in two dimensions, but others are relevant to the calculation of fluctuation corrections in general. Section V presents the results of including fluctuations, and discusses the effects of detuning and inhomogeneous broadening on the phase boundary. The discussion presented in Sec. V does not require the details presented in Sec. IV, and readers not interested in the theoretical explication may move directly to Sec. V. Finally, in Sec. VI we summarize our conclusions.

## II. MODEL

Our model describes localized two-level systems, coupled to a continuum of radiation modes in a two-dimensional microcavity. Considering only two levels describes a hard-core repulsion between excitons on a single site. If the on-site repulsion is large compared to other energy scales in the problem, it may be approximated by a hard-core repulsion between excitons, leading to a two-level description. We do not consider a static Coulomb interaction between different sites, nor the spin structure of the excitons, which could allow for multiple excitons per site. Such effects can be expected to make quantitative changes to, e.g., the transition temperature, but not to change the energy and length scales that control its value.

The two-level systems may either be represented as fermions with an occupancy constraint, as will be described below, or as spins with magnitude $|\mathbf{S}|=1/2$. In the latter case, the generalized Dicke Hamiltonian[28] is

$$H=\sum_{j=1}^{j=nA}2\epsilon_j S_j^z+\sum_{k=2\pi l/\sqrt{A}}\hbar\omega_k\psi_k^\dagger\psi_k + \frac{g}{\sqrt{A}}\sum_{j,k}(e^{2\pi i\mathbf{k}\cdot\mathbf{r}_j}\psi_k S_j^+ + e^{-2\pi i\mathbf{k}\cdot\mathbf{r}_j}\psi_k^\dagger S_j^-). \quad (1)$$

Here $A\to\infty$ is the quantisation area and $n$ the areal density of two-level systems, i.e., sites where an exciton may exist. Without inhomogeneous broadening, the energy of a bound exciton is $2\epsilon=\hbar\omega_0-\Delta$, defining the detuning $\Delta$ between the exciton and the photon. When later an inhomogeneously broadened band of exciton energies is introduced, $\Delta$ will represent the detuning between photon and center of the exciton band. The photon dispersion, for photons in an ideal two-dimensional (2D) cavity of width $w$, and relative permittivity $\varepsilon_r$ is

$$\hbar\omega_k=\hbar\frac{c}{\sqrt{\varepsilon_r}}\sqrt{k^2+\left(\frac{2\pi}{w}\right)^2}\approx\hbar\omega_0+\frac{\hbar^2k^2}{2m}, \quad (2)$$

so the photon mass is $m=(\hbar\sqrt{\varepsilon_r}/c)(2\pi/w)$.

The coupling constant $g$ written in the dipole gauge is

$$g=d_{ab}\sqrt{\frac{e^2}{2\varepsilon_0\varepsilon_r}\frac{\hbar\omega_k}{w}}, \quad (3)$$

where $d_{ab}$ is the dipole matrix element. For small photon wave vectors (with respect to $1/w$), it is justified to neglect the $k$ dependence of $g$, i.e., to take $\omega_k=\omega_0$. The factor of $1/\sqrt{w}$ is due to the quantization volume for the electric field.

The grand canonical ensemble, $\tilde{H}=H-\mu N$, allows the calculation of equilibrium for a fixed total number of excitations $N$ given by

$$N=\sum_{j=1}^{nA}\left(S_j^z+\frac{1}{2}\right)+\sum_{k=2\pi l/\sqrt{A}}\psi_k^\dagger\psi_k. \quad (4)$$

We therefore define $\hbar\tilde{\omega}_k=\hbar\omega_k-\mu$ and $\tilde{\epsilon}=\epsilon-\mu/2$. Expressing all energies in terms of the scale of the Rabi splitting $g\sqrt{n}$ and all lengths via the two-level system density $n$, there remain only two dimensionless parameters that control the system, the detuning $\Delta^*=\Delta/g\sqrt{n}$ and the photon mass $m^*=mg/\hbar^2\sqrt{n}$. Typical values for current experiments[3,5] are $g\sqrt{n}\approx 10$ meV, $m\approx 10^{-5}m_{\text{electron}}$, and taking $n\approx 1/a_{\text{Bohr}}^2\approx 10^{12}$ cm$^{-2}$ leads to an estimate of $m^*\approx 10^{-3}$.

This model is similar to that studied by Hepp and Lieb.[29] They considered the case $\mu=0$, i.e., without a bath to fix the total number of excitations. The transition studied by Hepp and Lieb was later shown by Rzążewski *et al.*[30] to be an artefact of neglecting $A^2$ terms in the coupling to matter. The transition in our model, when $\mu\neq 0$, does not suffer the same fate:[14] The sum rule of Rzążewski *et al.* which prevents condensation no longer holds when $\mu\neq 0$.

In order to integrate over the two-level systems, it is convenient to represent them as fermions, $S^z=\frac{1}{2}(b^\dagger b-a^\dagger a)$ and $S^+=b^\dagger a$. For each site there then exist four states, the two singly occupied states, $a^\dagger|0\rangle$, $b^\dagger|0\rangle$, and the unphysical states $|0\rangle$ and $a^\dagger b^\dagger|0\rangle$.

Following Popov and Fedotov[31] the sum over states may be restricted to the physical states by inserting a phase factor $e^{i(\pi/2)(b^\dagger b+a^\dagger a)}$. Since the Hamiltonian has identical expectations for the two unphysical states, this phase factor causes the contribution of zero occupied and doubly occupied sites to cancel, so the partition sum includes only physical states. Such a phase factor may then be incorporated as a shift of the Matsubara frequencies for the fermion fields, using instead $\omega_n=(n+3/4)2\pi T$. Thus from here we shall describe the two-level systems as fermions.

### A. High-energy properties, ultraviolet divergences

The Hamiltonian (1) is a low-energy effective theory, and will fail at high energies. This theory is not renormalizable; there exist infinitely many divergent one-particle irreducible diagrams, and so would need infinitely many renormalization conditions. These divergent diagrams lead to divergent expressions for the free energy and density.

To treat this correctly, it would be necessary to restore high-energy degrees of freedom, which lead to a renormalizable theory. Integrating over such high-energy degrees of freedom will recover, for low energies, the theory of Eq. (1). One may then calculate the free energy for the full theory, with appropriate counter terms. The low-energy contributions will be the same as before, but the high-energy parts differ, however, such high-energy parts are not relevant at low temperatures. As we are interested only in the low-energy properties of this theory, we will introduce a cutoff $K_{\mathrm{m}}$. The coupling $g$ is assumed to be zero between excitons and those photons with $k > K_{\mathrm{m}}$.

A number of candidates for this cutoff exist; the reflectivity bandwidth of the cavity mirrors, the Bohr radius of an exciton (where the dipole approximation fails), and the momentum at which photon energy is comparable to higher energy excitonic states (for which the two-level approximation fails). Which of these scales becomes relevant first depends on the exact system, however, changes in $K_{\mathrm{m}}$ will lead only to logarithmic errors in the density.

## III. MEAN-FIELD AND FLUCTUATION SPECTRUM

### A. Summary of mean-field results

We first briefly present the results of Refs. 14 and 16 for the mean-field analysis. Integrating over the fermion fields yields an effective action for photons:

$$S[\psi] = \int_0^\beta d\tau \sum_k \psi_k^\dagger (\partial_\tau + \hbar\tilde{\omega}_k)\psi_k + N\mathrm{Tr}\ln(\mathcal{M})$$

$$\mathcal{M}^{-1} = \begin{pmatrix} \partial_\tau + \tilde{\epsilon} & \frac{g}{\sqrt{A}}\sum_k e^{2\pi i \mathbf{k}\cdot\mathbf{r}_j}\psi_k \\ \frac{g}{\sqrt{A}}\sum_k e^{2\pi i \mathbf{k}\cdot\mathbf{r}_j}\psi_k^\dagger & \partial_\tau + \tilde{\epsilon} \end{pmatrix}. \quad (5)$$

We then proceed by minimizing $S[\psi]$ for a static uniform $\psi$ and expanding around this minimum. The minimum $\psi_0$ satisfies the equation

$$\hbar\tilde{\omega}_0\psi_0 = g^2 n \frac{\tanh(\beta E)}{2E}\psi_0, \quad E = \sqrt{\tilde{\epsilon}^2 + g^2\frac{|\psi_0|^2}{A}}. \quad (6)$$

which describe a mean-field condensate of coupled coherent photons and exciton polarization. The mean-field expectation of the density is given by

$$\rho_{\mathrm{M.F.}} = \frac{|\psi_0|^2}{A} + \frac{n}{2}\left[1 - \frac{\tilde{\epsilon}}{E}\tanh(\beta E)\right]. \quad (7)$$

Note that the photon field acquires an extensive occupation; we may define the intensive quantity $\rho_0 = |\psi_0|^2/A$: the density of photons in the condensate. This corresponds to an electric-field strength of $\sqrt{\hbar\omega_0\rho_0/2\varepsilon_0}$.

For an inhomogeneously broadened band of exciton energies, Eq. (6) should be averaged over exciton energies. In this case condensation will introduce a gap in the excitation spectrum of single fermions:[14] Whereas when uncondensed there may be single-particle excitations of energy arbitrarily close to the chemical potential, now the smallest excitation energy is $2g|\psi|/\sqrt{A}$. The existence of this gap is reflected by features of the collective-mode spectrum discussed below.

### B. Connection to Dicke superradiance

It is interesting to compare this mean-field condensed state, described by Eq. (6), to the superradiant state originally considered by Dicke.[28] Dicke considered a Hamiltonian similar to Eq. (1), but with a single photon mode. Constructing eigenstates $|L,m\rangle$ of the modulus and $z$ component of the total spin, $\mathbf{S} = \Sigma_j \mathbf{S}_j$, Dicke showed that for $N$ particles, the state $|N/2,0\rangle$ has the highest radiation rate.

Taking the state described by the mean-field condensate, Eq. (6), and considering the limit as $\psi_0 \to \infty$ and $T \to 0$, the equilibrium state may be written as

$$|\psi_{\mathrm{cond.}}\rangle = \frac{1}{2^{N/2}}\prod_j (|\uparrow\rangle_j + |\downarrow\rangle_j) \quad (8)$$

$$= \frac{1}{2^{N/2}}\sum_{p=0}^{N}\sqrt{\binom{N}{p}}\left|\frac{N}{2},\frac{N}{2}-p\right\rangle, \quad (9)$$

i.e., a binomial distribution of angular momentum states.

As $N$ tends to infinity, this becomes a Gaussian centered on the Dicke super-radiant state, with a width that scales like $\sqrt{N}$. However, it should be noted that the above state represents only the exciton part; this should be multiplied by a photon coherent state. In the self-consistent state, there exists a sum of terms with different divisions of excitation number between the photons and excitons. These different divisions have a fixed phase relationship. Such a statement would remain true even if projected onto a state of fixed total excitation number. This is different from the Dicke superradiant state, which has no photon part. In the Dicke state, the only important coherence is that between the different ways of distributing excitations between the two-level systems.

### C. Comparison of mean-field results with other boson-fermion systems

The mean-field equations (6) and (7) have a form that is common to a wide range of fermion systems. However, the form of the density of states and the nature of fermion interactions can significantly alter the form of the mean-field phase boundary. It is of interest to compare our system to other systems in which BCS-BEC crossover has been considered, and to note that even at the mean-field level, important differences emerge. To this end, we compare the mean-field equations for our modified Dicke model to the Holland-Timmermans Hamiltonian,[25–27] and to BCS superconductivity.[32]

For a gas of Fermionic atoms, or BCS, the density of states is nonzero for all energies greater than zero, whereas for our localized excitons, without inhomogeneous broadening, it is a $\delta$ function. One immediate consequence is a difference of interpretation of the mean-field equations; the number equation and the self-consistent condition for the

anomalous Green's function. For a weakly interacting fermion system the number equation alone fixes the chemical potential,[33] and the self-consistent condition can then be solved to find the critical temperature. For our localized fermions, the chemical potential lies below the band of fermions, and so the density is controlled by the tail of the Fermi distribution, so temperature and chemical potential cannot be so neatly separated. This can remain true even in the presence of inhomogeneous broadening; the majority of density may come from regions of large density of states in the tail of the Fermi distribution.

Such differences are also reflected in the density dependence of the mean-field transition. The absence of a direct four-fermion interaction means that the effective interaction strength is entirely due to photon mediated interactions. Since our model has the photons at chemical equilibrium with the excitons, this effective interaction strength depends strongly upon the chemical potential.

For BCS superconductors, and the BCS limit for weakly interacting Fermionic atoms, the dependence of critical temperature upon density is due to the changing density of states, which appears in the self-consistent equation as a prefactor of the logarithm in the BCS equation $1/g = \rho_s \ln(\omega_D/T_c)$. In contrast, the density dependence of $T_c$ for the Dicke model is due to the changing coupling strength and occupation of two-level systems with changing chemical potential. Such a change of coupling strength with chemical potential also occurs in the Holland-Timmermans model, near Feshbach resonance, where the boson mediated interaction is not dominated by the direct four-fermion term. Even with inhomogeneous broadening of energies, unless the chemical potential remains fixed at low densities, there will be a strong density dependence of $T_c$ as the effective interaction strength changes. The resultant phase boundary with inhomogeneous broadening, at low densities, is given in Sec. V C.

### D. Effective action for fluctuations

Including fluctuations about the saddle point, $\psi = \psi_0 + \delta\psi$, one may write the two-level system inverse Green's function as $\mathcal{M}^{-1} = \mathcal{M}_0^{-1} + \delta\mathcal{M}^{-1}$, where

$$\delta\mathcal{M}^{-1} = \frac{g}{\sqrt{A}} \sum_k \begin{pmatrix} 0 & e^{2\pi i \mathbf{k}\cdot\mathbf{r}_j}\delta\psi_k \\ e^{-2\pi i \mathbf{k}\cdot\mathbf{r}_j}\delta\bar{\psi}_k & 0 \end{pmatrix}, \tag{10}$$

thus Eq. (5) can be expanded to quadratic order as

$$S = S[\psi_0] + \beta \sum_{i\omega} \sum_k (i\omega + \hbar\tilde{\omega}_k) |\delta\psi_{\omega,k}|^2 - \frac{N}{2} \mathrm{Tr}(\mathcal{M}_0 \delta\mathcal{M}^{-1} \mathcal{M}_0 \delta\mathcal{M}^{-1}) \tag{11}$$

$$= S[\psi_0] + \frac{\beta}{2} \sum_{i\omega} \sum_k (\delta\bar{\psi}_{\omega,k}, \delta\psi_{-\omega,-k}) \times \begin{pmatrix} i\omega + \hbar\tilde{\omega}_k + K_1(\omega) & K_2(\omega) \\ K_2^*(\omega) & -i\omega + \hbar\tilde{\omega}_k + K_1^*(\omega) \end{pmatrix} \begin{pmatrix} \delta\psi_{\omega,k} \\ \delta\bar{\psi}_{-\omega,-k} \end{pmatrix}. \tag{12}$$

The matrix between the photon fields can be identified as the inverse of the fluctuation photon Green's function, $\mathcal{G}^{-1}$, where the exciton contribution to the quadratic term [with $\nu = (n+3/4)2\pi T$] is

$$K_1(\omega) = \frac{g^2}{A} \sum_j \sum_\nu \frac{(i\nu + \tilde{\epsilon})(i\nu + i\omega - \tilde{\epsilon})}{(\nu^2 + E^2)[(\nu+\omega)^2 + E^2]} = g^2 n \frac{\tanh(\beta E)}{E} \left( \frac{i\tilde{\epsilon}\omega - E^2 - \tilde{\epsilon}^2}{\omega^2 + 4E^2} \right) |\alpha| \delta_\omega, \tag{13}$$

$$K_2(\omega) = \frac{g^2}{A} \sum_j \sum_\nu \frac{g^2\psi_0^2/A}{(\nu^2 + E^2)[(\nu+\omega)^2 + E^2]} = g^2 n \frac{\tanh(\beta E)}{E} \left( \frac{g^2\psi_0^2/A}{\omega^2 + 4E^2} \right) - \alpha\delta_\omega, \tag{14}$$

$$\alpha = g^2 n \beta \frac{\mathrm{sech}^2(\beta E)}{4E^2} g^2 \frac{\psi_0^2}{A}, \tag{15}$$

where the sum over sites assumed no inhomogeneous broadening, and $\omega$ is a Bosonic Matsubara frequency $2\pi nT$. The mean-field action $S[\psi_0]$, is given by

$$S[\psi_0] = \hbar\tilde{\omega}_k |\psi_0|^2 - \frac{\mu N}{2} - \frac{N}{\beta} \ln[\cosh(\beta E)]. \tag{16}$$

The terms $\alpha\delta_\omega$ occur when the sum over Fermionic frequencies in Eqs. (13) and (14) have second-order poles. These terms must be included in the thermodynamic Green's function at $\omega = 0$. However, they do not survive analytic continuation, and so do not appear in the retarded Green's function or in the excitation spectrum. This is discussed in the Appendix.

Even considering inhomogeneous broadening of exciton energies, such terms remain as $\delta_\omega$, rather than some broadened peak. This can be understood by considering which transitions contribute to the excitons' response to a photon, i.e., between which exciton states there is a matrix element due to the photon. If uncondensed, the photon couples to transitions between the exciton's two energy states, $\pm\epsilon$. In the presence of a coherent field, these energy states mix. The photon then couples both to transitions $E \to -E$ and also to the degenerate transition $E \to E$. Since this transition is between the two levels on a single site, inhomogeneous broadening does not soften the $\delta_\omega$ term.

This conclusion differs for models with transitions between two bands of fermion states. If transitions are allowed between any pair of lower and upper band states, the degenerate transition above is replaced by a continuum of intraband transitions. In our model all intraband excitations are of zero energy. If there exists a range of low-energy intraband transitions, these allow the Goldstone mode to decay, giving rise to Landau damping.[27,34] For our model, as there is no continuum of modes, no such damping occurs.

In order to consider fluctuations for an inhomogeneously broadened system of excitons, a correct treatment requires calculating for a given realization of disorder, and then averaging the final results. Because the position of an exciton matters in its coupling to light, it would be necessary to

include averaging over disorder in both energy and position of excitons. However, for low-energy modes, we may make an approximation, and average the expressions for $K_1, K_2$ over exciton energies.

This approximation is equivalent to the assumption that the energies and positions of excitons sampled by photons of different momenta are independent and uncorrelated. Such an approximation evidently cannot hold for high momenta, as otherwise the number of random variables would become greater than the number of excitons. This approximation will also necessarily neglect scattering between polariton momenta states. However, such effects involve high-energy states (since they require momenta on the order of the inverse exciton spacing), and can be neglected in discussing the low-energy behavior.

### E. Fluctuation spectrum

Inverting the matrix in the effective action for fluctuations, Eq. (12), one finds the fluctuation Green's function. The location of the poles of this Green's function give the spectrum of those excitations which can be created by injecting photons, measured relative to the chemical potential.

These poles come from the denominator:

$$\det(\mathcal{G}^{-1}) = |i\omega + \hbar\tilde{\omega}_k + K_1(\omega)|^2 - |K_2(\omega)|^2 = \frac{(\omega^2+\xi_1^2)(\omega^2+\xi_2^2)}{(\omega^2+4E^2)}, \tag{17}$$

where, as discussed above, we have ignored the $\delta_\omega$ terms, and assumed no inhomogeneous broadening of excitons.

In the condensed state the poles are

$$\xi_{1,2}^2 = \frac{1}{2}\{A(k) \pm \sqrt{A(k)^2 - B(k)}\}, \tag{18}$$

where

$$A(k) = 4E^2 + (\hbar\tilde{\omega}_k)^2 + 4\tilde{\epsilon}\hbar\tilde{\omega}_0, \tag{19}$$

$$B(k) = 16\frac{\hbar^2k^2}{2m}(E^2\hbar\tilde{\omega}_k - \tilde{\epsilon}^2\hbar\tilde{\omega}_0). \tag{20}$$

In the normal state this simplifies further, $K_2$ is zero, and Eq. (17) is replaced by

$$|i\omega + \hbar\tilde{\omega}_k + K_1(\omega)|^2 = \left|\frac{(i\omega+E_+)(i\omega+E_-)}{(i\omega+2\tilde{\epsilon})}\right|^2. \tag{21}$$

There are two poles, the upper and lower polariton:

$$E_\pm = \frac{1}{2}[(\hbar\tilde{\omega}_k + 2\tilde{\epsilon}) \pm \sqrt{(\hbar\tilde{\omega}_k - 2\tilde{\epsilon})^2 + 4g^2n\tanh(\beta\tilde{\epsilon})}]. \tag{22}$$

The polariton dispersion (22) from localized excitons has the same structure as from propagating excitons, since the photon dispersion dominates. The spectra, both condensed and uncondensed, are shown in Fig. 1. For a model of dispersive, Bosonic excitons, the equivalent of Eq. (22) has a similar form, but with $2\tilde{\epsilon} \to 2\tilde{\epsilon} + k^2/2m_{\rm ex}$. Over the momentum range

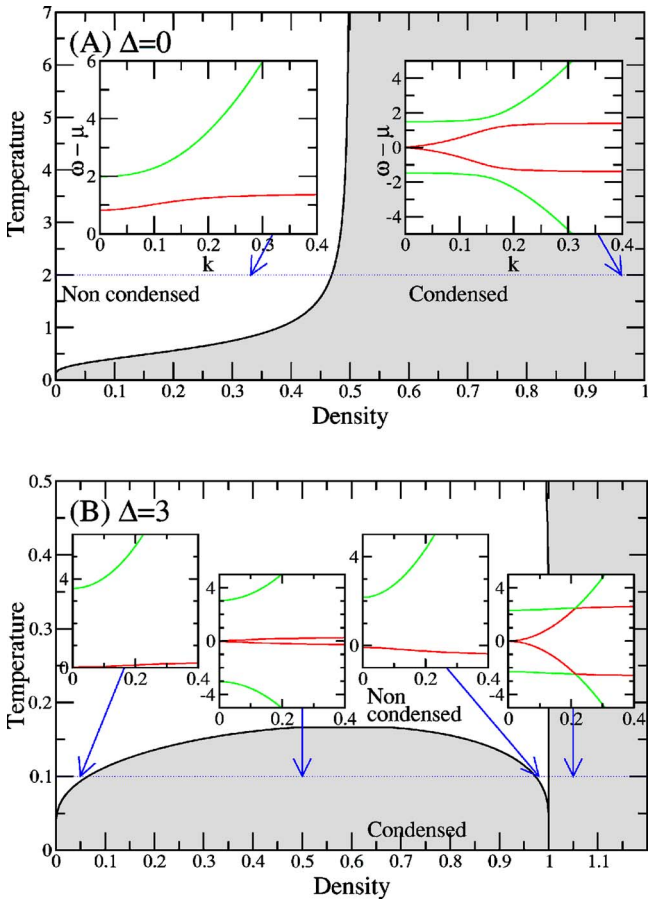


FIG. 1. (Color online) Excitation spectra in the condensed (grey) and uncondensed states, superimposed on the mean-field phase diagram, to show choice of density and temperature. Panel A is for the photon and exciton resonant, and the two spectra are for $T=2g\sqrt{n}$ and $\mu/g\sqrt{n}=-1.4$ and $-0.24$. Panel B has the exciton detuned by $3g\sqrt{n}$ below the photon, and the spectra are for $T=0.1g\sqrt{n}$ and $\mu/g\sqrt{n}=-3.29$, $-3.01$, $-2.54$, and $-0.37$. The photon mass is $m^*=0.01$. Temperatures and energies plotted in units of $g\sqrt{n}$, densities in units of $n$, and wave vectors in units of $\sqrt{n}$.

in Fig. 1, the exciton dispersion would lead to a shift of exciton energy of the order of $10^{-3}g\sqrt{n}$, i.e., negligible over the entire scale of Fig. 1.

The difference between condensed and uncondensed spectra is dramatic: two new poles appear. These arise because the off diagonal terms in Eq. (12) mix photon creation and annihilation operators. Such a spectrum may be observed in polariton condensation experimentally, as one may probe the response to inserting a real photon, and observing its emission at a later time. In the presence of a condensate, the polariton is not a quasiparticle. Creating a photon corresponds to a superposition of creating and destroying quasiparticles. At nonzero temperature, a population of quasiparticles exists, so processes where a quasiparticle is destroyed is possible. This means that a process in which a photon, with energy less than the chemical potential, is added to the system is possible [i.e., $P_{\rm absorb}$ as defined in Eq. (A7)]. However, if the system is experimentally probed with photons of energy less than the chemical potential, what will be observed is gain, since the absorption of photons is more than

canceled by spontaneous and stimulated emission.

At small momentum, $\xi_1$ corresponds to phase fluctuations of the condensate, i.e., it is the Goldstone mode, and has the form $\xi_1 = \pm \hbar c k$, with

$$c = \sqrt{\frac{1}{2m}\left(\frac{4\hbar\tilde{\omega}_0 g^2 n}{\xi_2(0)^2}\right)\left(\frac{|\psi_0|^2}{N}\right)} \approx \sqrt{\frac{\lambda}{2m}\frac{\rho_0}{n}}. \quad (23)$$

The second expression is, for comparison, the form of the Bogoliubov mode in a dilute Bose gas, of interaction strength $\lambda$. As $\psi_0$ increases, the phase velocity first increases, then decreases. The decrease is due to the saturation of the effective exciton-photon interaction.

The leading-order corrections $\xi_1 = \pm ck + \alpha k^2$ are of interest for considering Beliaev decay of phonons.[35]. If $\alpha < 0$, kinematic constraints prevent the decay of phonons. For the Bogoliubov spectrum in a dilute Bose gas, $\alpha = 0$, and the cubic term becomes relevant. Here, both signs are possible, according to whether the spectrum crosses over to the quadratic lower polariton dispersion before this crosses over to a flat exciton dispersion. In most cases, $\alpha > 0$ and $\xi_1$ will have a point of inflection, but if the exciton is detuned below the photon, then for certain densities, $\alpha < 0$, and the curvature is always negative.

The modes may also be compared to the Cooperon modes in BCS theory. At small momenta, although the mode $\xi_1$ becomes a pure phase fluctuation, the other mode $\xi_2$ is not an amplitude fluctuation. To see why this is so, it is helpful to rewrite the action in Eq. (12) in terms of the Fourier components of the transverse and longitudinal fluctuations of the photon field. These components, at quadratic order, are equivalent to the phase and amplitude components, and are given by

$$\delta\psi_{\omega,k} = \psi_L(\omega,k) + i\psi_T(\omega,k),$$

$$\delta\bar{\psi}_{\omega,k} = \psi_L(-\omega,-k) - i\psi_T(-\omega,-k). \quad (24)$$

In terms of these new variables, the action may be written

$$S = S[\psi_0] + \beta\sum_{i\omega,k}(\psi_L(-\omega,-k)\psi_T(-\omega,-k)) \times \begin{pmatrix} \hbar\tilde{\omega}_k + \mathrm{Re}(K_1) + K_2 & -\omega - \mathrm{Im}(K_1) \\ \omega + \mathrm{Im}(K_1) & \hbar\tilde{\omega}_k + \mathrm{Re}(K_1) - K_2 \end{pmatrix}\begin{pmatrix} \psi_L(\omega,k) \\ \psi_T(\omega,k) \end{pmatrix}. \quad (25)$$

Due to the off-diagonal components, the eigenstates are mixed amplitude and phase modes. This mixing vanishes only where $\omega$ is small, which means that the lowest energy parts of the Goldstone mode are purely phase fluctuations. Since the amplitude mode at $k=0$ has a nonzero frequency, it will mix with the phase mode.

The off diagonal terms come from two sources. The dynamic photon field leads to the term $\omega$. The fermion mediated term $\mathrm{Im}(K_1)$ will be nonzero if the density of states is asymmetric about the chemical potential. For the Dicke model, both terms contribute to mixing since

$$\mathrm{Im}(K_1) = g^2 n\frac{\tanh(\beta E)}{E}\left(\frac{\tilde{\epsilon}\omega}{\omega^2 + 4E^2}\right). \quad (26)$$

Unless $\tilde{\epsilon}=0$, the density of states is not symmetric about the chemical potential, and so this term is nonzero.

For BCS superconductivity the pairing field is not dynamic, so there is no off-diagonal $\omega$ term. However, there can still be mixing due to $\mathrm{Im}(K_1)$, which is given by

$$\mathrm{Im}(K_1) = \sum_{i\nu,q}\frac{\nu(\epsilon_q - \epsilon_{q+Q}) + \omega\epsilon_q}{(\nu^2 + \epsilon_q^2 + \Delta^2)[(\nu+\omega)^2 + \epsilon_{q+Q}^2 + \Delta^2]}, \quad (27)$$

in which $\nu$ is a Fermionic Matsubara frequency, $(2n+1)\pi T$, and $\Delta$ the superconducting gap. Note that this coupling now depends on the momentum transfer $Q$ as well as energy $\omega$. If the density of states is symmetric, e.g., $\epsilon_q = v_F q$, then at $Q=0$, $\mathrm{Im}(K_1)$ will be zero, and as the boson field has no dynamics, the modes will then entirely decouple. In real superconductors, symmetry of the density of states about the chemical potential is only approximate, and so some degree of mixing will occur.

### F. Luminescence spectrum

Although four poles exist, they may have very different spectral weights. At high momentum, the weights of all poles except the highest vanish, and the remaining pole follows the bare photon dispersion.

Such effects can be seen more clearly by plotting the incoherent luminescence spectrum. As discussed in the Appendix, this can be found from the Green's function as

$$P_{\mathrm{emit}}(x) = 2n_B(x)\mathrm{Im}[\mathcal{G}_{00}(i\omega = x + i\eta)]. \quad (28)$$

It is easier to observe how the spectral weight associated with poles changes after adding inhomogeneous broadening. Figure 2 plots the luminescence spectrum for the same parameters as in Fig. 1, but with inhomogeneous broadening. This will broaden the poles, except for the Goldstone mode [labeled (d) in Fig. 2], as discussed above. The distribution of energies used is, for numerical efficiency, a cubic approximation to a Gaussian, with standard deviations $0.1g\sqrt{n}$ and $0.3g\sqrt{n}$. The results with a Gaussian density of states have been compared to this cubic approximation, and no significant differences occur.

In the condensed case, a third pair of lines are visible, [labeled (c) in Fig. 2]. These correspond to the minimum energy for a neutral excitation, $2g\sqrt{n}\psi_0$, i.e., flipping the spin on a single site. They are analogous to a particle-hole excitation in BCS, which have twice the energy of the gap for adding a single particle. This energy is the smallest "interband excitation." If the inhomogeneous broadening is small compared to the gap then these extra lines will be less visible, as seen in Fig. 2(B). For large inhomogeneous broadening, the peak at the edge of the gap (c) and the upper polariton (b) will merge, as shown by (e) in Fig. 2(D). This will result in a band of incoherent luminescence separated from the coherent emission at the chemical potential by the gap. Such structure, although associated with the internal structure of a polariton, can be seen even at densities where the

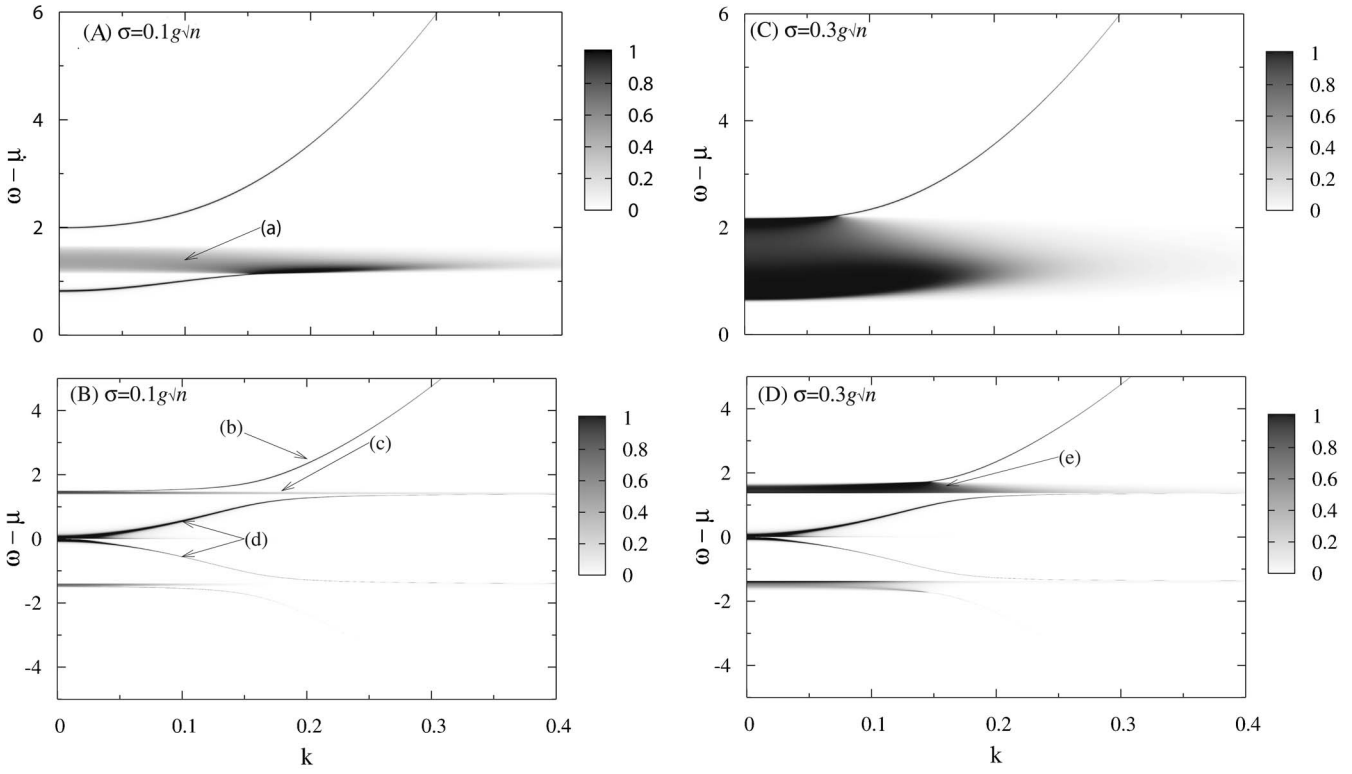


FIG. 2. Incoherent luminescence vs momentum ($x$ axis) and energy ($y$ axis) calculated above [panels (A) and (C)] and below [panels (B) and (D)] phase transition. Panels (A) and (B) are for inhomogeneous broadening of $0.1g\sqrt{n}$, and (C) and (D) are for $0.3g\sqrt{n}$. All other parameters are the same as in the unbroadened case shown in panel (A) of Fig. 1. In order to map the infinite range of intensities to a finite scale, the color is allocated as the hyperbolic tangent of intensity. Energies are in units of $g\sqrt{n}$, and wave vectors in units of $\sqrt{n}$.

transition temperature is adequately described by a model of structureless polaritons.

It is also interesting to consider the uncondensed cases. In Fig. 2(A), with the smaller broadening, three lines are visible; the upper and lower polariton, and between them luminescence from excitons weakly coupled to light [labeled (a)]. These weakly coupled states arise from excitons further away from resonance with the photon band. Although there may be a large density of such states, they make a much smaller contribution to luminescence than the polariton states, because of their small photon component. With larger broadening, these weakly coupled excitons form a continuum stretching between the two modes, as shown in Fig. 2(C).

### G. Momentum distribution of photons

From the Green's function for photon fluctuations, one can calculate the momentum distribution of photons in the cavity. For a two-dimensional cavity coupled via the mirrors to three-dimensional photons outside, the momentum distribution may be observed experimentally from the angular distribution.[3]

When uncondensed, $N(p)$ is given by

$$N(p) = \lim_{\delta\to 0^+} \langle \psi_p^\dagger(\tau+\delta)\psi_p(\tau)\rangle = \lim_{\delta\to 0^+} \beta \oint \frac{dz}{2\pi i} n_B(z) e^{\delta z} \mathcal{G}_{11}(iz,p). \quad (29)$$

However, when condensed, since the system is two dimensional, it is necessary to treat fluctuations more carefully. Writing $\psi(r)=\sqrt{\rho_0+\pi(r)}e^{i\phi(r)}$, the action involves only derivatives of the phase, showing that large phase fluctuations are possible. For quadratic fluctuations, one can use the matrix in Eq. (25) describing transverse and longitudinal modes, and relate these to the phase and amplitude excitations.

At low enough temperatures, it is possible to calculate $N(p)$ by considering only the phase mode.[36] Thus neglecting amplitude fluctuations gives

$$N(p) = \frac{1}{A}\int d^2r \int d^2r' e^{i\mathbf{k}\cdot(\mathbf{r}-\mathbf{r}')}\rho_0\langle e^{i[\phi(\mathbf{r})-\phi(\mathbf{r}')]}\rangle = \rho_0 \frac{1}{A}\int d^2R \int d^2t e^{i\mathbf{k}\cdot\mathbf{t}} e^{-D(\mathbf{R}+\mathbf{t}/2,\mathbf{R}-\mathbf{t}/2)}, \quad (30)$$

where $\rho_0$ is taken as the mean-field photon density. The phase correlator, found by inverting the amplitude-phase action, is

$$D(\mathbf{r},\mathbf{r}') = \int \frac{d^2k}{(2\pi)^2}\{1-\cos[\mathbf{k}\cdot(\mathbf{r}-\mathbf{r}')]\}\frac{m}{\beta\rho_0\hbar^2k^2} \approx \frac{m}{2\pi\beta\rho_0\hbar^2}\ln\left(\frac{|\mathbf{r}-\mathbf{r}'|}{\xi_T}\right). \quad (31)$$

The thermal length is $\xi_T=\beta c$, where $c$ is the velocity of the sound mode from Eq. (23). This comes from the energy scale

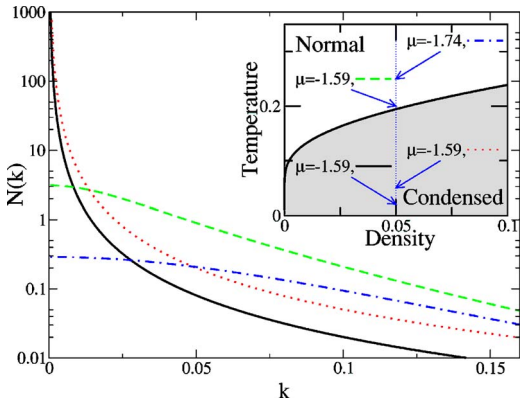


FIG. 3. (Color online) Momentum distribution of photons, from which follows the angular distribution. These are plotted for low-temperature condensed systems, where the approximation of including only phase fluctuations is valid, and for the simpler, uncondensed case. The inset illustrates the choices of density and temperature. (Parameters are $\Delta^*=1$, $m^*=0.01$, wave vector plotted in units of $g\sqrt{n}$, temperature in units of $g\sqrt{n}$, density in units of $n$, and $N(k)$ in arbitrary units.)

at which fluctuations become cut by the thermal distribution.

In this approximation, Eq. (30) may be evaluated exactly[37] giving

$$N(p) = 2\pi\rho_0 \frac{(p\xi_T)^\eta}{p^2} \int_0^\infty x^{1-\eta} J_0(x) dx$$

$$= 2\pi\rho_0 \frac{\xi_T^\eta}{p^{2-\eta}} 2^{1-\eta} \frac{\Gamma(1-\eta/2)}{\Gamma(\eta/2)}, \tag{32}$$

where $\eta = m/2\pi\beta\rho_0\hbar^2$ controls the power-law decay of correlations. The second line follows from an identity (see Ref. 38, exercise XVII.32). This is valid only for small $\eta$, far from the transition. The Kosterlitz-Thouless transition[39] occurs when $\eta$ becomes large, an approximate estimate of the transition is at $\eta=2$.

The momentum distribution can therefore be calculated both at low temperatures, where such a scheme holds, and at high temperatures, when uncondensed. This is shown in Fig. 3. When condensed, the power-law divergence leads to a peak normal to the plane. This peak reflects coherence between distant parts of the system, so in a finite system this peak is cut at small momenta.[36]

## IV. FLUCTUATION CORRECTION TO THE MEAN-FIELD THEORY

In this section, we calculate the fluctuation corrections to the mean-field density, and thus to the mean-field phase boundary. Our method is similar to that of Nozières and Schmitt-Rink,[40] who studied fluctuation corrections to the BCS mean-field theory for a model of interacting, propagating fermions. However, because our model differs from that of Nozières and Schmitt-Rink, our approach to including second-order fluctuations will also differ. We begin by presenting a brief summary of the method used by Nozières and Schmitt-Rink, and further developed by Randeria.[33] We then discuss how our approach differs from their work.

### *1. Fluctuation corrections in three dimensions*

To consider fluctuation corrections to a mean-field theory, one first needs to find the partition function in terms of a coherent-state path integral for a Bosonic field,

$$\mathcal{Z} = \int \mathcal{D}\psi \exp(-S[\psi]).$$

For the Dicke model, $S[\psi]$ is given in Eq. (5). In the work of Nozières and Schmitt-Rink, $S[\psi]$ resulted from decoupling a four-fermion interaction, and then integrating over the fermions. This effective action may be understood as a Ginzburg-Landau theory, with coefficients that are functions of temperature and chemical potential as well as the parameters in the Hamiltonian. To find the mean-field phase boundary, one needs both to find the values of temperature and chemical potential where the transition occurs, and to calculate the density evaluated at these parameters.

For the mean-field theory, the action is evaluated for a static uniform field, $\psi_0$, and minimized with respect to this field. At the critical temperature, a second-order phase transition occurs, and the minimum action moves to a nonzero $\psi_0$. The density is found by differentiating the free energy with respect to chemical potential. For the mean-field theory, the free energy is approximated by the action evaluated at $\psi_0$.

To go beyond the mean-field theory, one can expand the effective action about the saddle point:

$$\mathcal{Z} \approx e^{-S[\psi_0]} \int \mathcal{D}\delta\psi \exp\left(-\frac{1}{2}\left.\frac{\partial^2 S}{\partial\psi^2}\right|_{\psi_0} (\delta\psi)^2\right). \tag{33}$$

This gives an improved estimate of the free energy, from which follows an improved estimate of the density, and thus of the phase boundary. In three dimensions (but not in two, as discussed below), one only needs an estimate of the density at the mean-field critical temperature. It is therefore sufficient to consider an expansion about the normal-state saddle point, $\psi=0$. Such fluctuations may be understood as the contribution to the density from noncondensed pairs of particles, whereas the mean-field estimate of density included only unpaired fermions. These corrections will increase the density at a fixed critical temperature, or equivalently decrease the critical temperature for a given density.

Because of features of our model, our approach differs from that of Nozières and Schmitt-Rink; two differences in our model are of particular importance. First, our boson field is dynamic, and there exists a chemical potential for bosons. In this respect, our model is closer to the boson-fermion models[25,26] studied in the context of Feshbach resonances, for which Ohashi and Griffin[27] have studied fluctuation corrections. Second, we consider a two-dimensional system; this requires calculation of fluctuations in the presence of a condensate, as discussed in the next section.

### *2. Fluctuations in two dimensions*

To find the fluctuation correction to the mean-field phase boundary in two dimensions, it is necessary to consider fluc-

tuations in the presence of a condensate. Considering fluctuations in the normal state would lead to the conclusion that the normal state can support any density: As one approaches the mean-field critical temperature, the fluctuation density will become infrared divergent, allowing any density. This correctly indicates that no long-range order exists in two dimensions; however, a Kosterlitz-Thouless[39,41] transition does occur.

Instead one must start by considering fluctuations in the presence of a condensate. This gives a density, defined by the total derivative of free energy with respect to chemical potential, of the form

$$\rho = -\frac{dF}{d\mu} = -\frac{\partial F}{\partial \mu} - \frac{\partial F}{\partial \psi_0}\frac{d\psi_0}{d\mu}. \tag{34}$$

When considering fluctuation corrections in the presence of a condensate, in any dimension, one must take care to consider the depletion of the order parameter due to the interaction between condensed and uncondensed particles. This is discussed in detail in Sec. IV A. Such a depletion means that, for a fixed temperature, the critical value of the chemical potential changes; at the mean-field critical chemical potential the formula for total density may become negative. It is therefore necessary to make a separate estimate of the order parameter in the presence of fluctuations, and define the phase boundary where the order parameter goes to zero.

In three dimensions such a calculation can be achieved by identifying parts of the density as the population of the ground state and of fluctuations (as discussed below in Sec. IV A 2b). In two dimensions, no true condensate exists, but a quasicondensate with a cutoff $k_0$ can be considered. As discussed by Popov,[42] the quasicondensate and fluctuation densities both contain terms which diverge logarithmically as $k_0 \to 0$, but these divergences cancel in the total density.

Instead, in two dimensions, one must consider an alternate definition for the location of the phase boundary. Since the transition is a Kosterlitz-Thouless transition, one should map the problem to the two-dimensional Coulomb gas.[43] This requires the vortex core energy and strength of vortex-vortex interactions, which both scale as $\hbar^2\rho_s/2m$, where $\rho_s$ is a superfluid response density. The phase transition thus occurs when $\rho_s = \#2mT/\hbar^2$. The numerical prefactor depends on the vortex core structure. However, approximating the critical condition by $\rho_s = 0$ leads to only a small shift to $T_C$.

### A. Total derivatives and negative densities

This section discusses the effects and interpretation of the second term in Eq. (34). In Eq. (3.41) of Ref. 27, Ohashi and Griffin define the density as the partial derivative of free energy with respect to chemical potential, neglecting the second term in Eq. (34), which they describe as a higher-order correction under the Gaussian fluctuation approximation. As shown below in Sec. IV A 1, the contribution of the second term in Eq. (34) to the density should not necessarily be neglected in the Gaussian fluctuation approximation. Section IV A 2 shows explicitly that the two terms in Eq. (34) are of the same order. The existence of the second term is crucial in finding a finite density in two dimensions, however, may be less important in three dimensions.

#### *1. Gaussian fluctuation approximation*

In Sec. IV A 2 we will show that the second term in Eq. (34) is of the same order as the first. Before this, we explain why the second term of Eq. (34) should not be automatically neglected. Even though it is of the form $\partial^3 S/\partial\psi_0^3$, such terms are not necessarily small, and can contribute to the density at quadratic order.

To see that a Gaussian theory may be correct even if such third-order terms are not small, consider an expansion of the effective action,

$$S = S[\psi_0] + \frac{d^2S}{d\psi_0^2}\delta\psi^2 + \frac{d^3S}{d\psi_0^3}\delta\psi^3 + \cdots. \tag{35}$$

A Gaussian approximation is justified if, using this action, the expectation of the cubic term is less than the quadratic term. This condition can be written as

$$\left(\frac{d^2S}{d\psi_0^2}\right)^{3/2} \gg \frac{d^3S}{d\psi_0^3}. \tag{36}$$

This need not require that the coefficient of the cubic term is smaller, i.e., that

$$\frac{d^2S}{d\psi_0^2} \gg \frac{d^3S}{d\psi_0^3}.$$

In fact, if both terms are of the same order, but large; $d^2S/d\psi_0^2 \simeq d^3S/d\psi_0^3 \gg 1$, then the condition (36) is fulfilled.

Writing the free energy including fluctuations schematically as

$$F = S[\psi_0] + \ln\left[\int \mathcal{D}\delta\psi \exp\left(-\frac{d^2S}{d\psi_0^2}\delta\psi^2\right)\right], \tag{37}$$

the fluctuation contribution to the second term in Eq. (34) will take the form

$$\rho = \cdots + \left\langle \frac{d^3S}{d\psi_0^3}\delta\psi^2 \right\rangle \frac{d\psi_0}{d\mu}, \tag{38}$$

where $\langle\cdots\rangle$ signifies averaging over the fluctuation action. Thus in calculating the condensate density, there is a term which depends on $\partial^3 S/\partial\psi_0^3$ but only involves second-order expectations of the fields. Since $\partial^3 S/\partial\psi_0^3$ is not necessarily small, and it contributes to the density at quadratic order, there is no *a priori* argument for neglecting this term. In the following we show explicitly that this term should be included.

#### *2. Total derivatives for a dilute Bose gas*

The following discussion will show explicitly that the two terms in Eq. (34) are of the same order for a weakly interacting dilute Bose gas (WIDBG),

$$H-\mu N=\sum_k(\epsilon_k-\mu)a_k^\dagger a_k+\frac{g}{2}\sum_{k,k',q}a_{k+q}^\dagger a_{k'-q}^\dagger a_k a_{k'}. \quad (39)$$

Further, the terms in Eq. (34) will be interpreted by considering the Hugenholtz-Pines relation at one loop order, as discussed in Ref. 42.

*Saddle point and fluctuations* To find the free energy, consider the static uniform saddle point, $\langle a_0^\dagger a_0\rangle=|A|^2=\mu/g$, and quadratic fluctuations, which are governed by the Hamiltonian

$$H_{\text{eff}}=\sum_k(\epsilon_k-\mu+2gA^2)a_k^\dagger a_k+\frac{gA^2}{2}(a_k^\dagger a_{-k}^\dagger+a_k a_{-k}). \quad (40)$$

Thus by a Bogoliubov transform, the free energy and density become

$$F=-\mu A^2+\frac{g}{2}A^4+\sum_k\left(\frac{1}{\beta}\ln(1-e^{-\beta E_k})+\frac{1}{2}(E_k-\epsilon_k-\mu)\right), \quad (41)$$

$$\rho=A^2-\sum_k\left(n_B(E_k)\frac{\epsilon_k}{E_k}+\frac{\epsilon_k-E_k}{2E_k}\right), \quad (42)$$

where $E_k=\sqrt{\epsilon_k(\epsilon_k+2\mu)}$.

The total density is thus less than the saddle point $A^2$, and could be negative. From the form of the fluctuation Hamiltonian, Eq. (40), using $gA^2=\mu$, it can be seen that the fluctuation contribution is

$$\rho_f=-\sum_k\left\{\langle a_k^\dagger a_k\rangle+\frac{1}{2}(\langle a_k^\dagger a_{-k}^\dagger\rangle+\langle a_k a_{-k}\rangle)\right\}. \quad (43)$$

Using the results

$$\langle a_k^\dagger a_k\rangle=n_B(E_k)\frac{\epsilon_k+\mu}{E_k}+\frac{\epsilon_k+\mu-E_k}{2E_k}, \quad (44)$$

$$\langle a_k^\dagger a_{-k}^\dagger\rangle=\langle a_k a_{-k}\rangle=-\frac{\mu}{E_k}\left(n_B(E_k)+\frac{1}{2}\right), \quad (45)$$

it is clear this matches Eq. (42).

In contrast, taking partial derivatives, and neglecting the second term in Eq. (34) gives $\rho_f=\Sigma_k\langle a_k^\dagger a_k\rangle$. In two dimensions, for $\mu\neq 0$, this expression will be infrared divergent, while Eq. (42) is not.

*Hugenholtz-Pines relation* To identify the meaning of the terms in Eq. (43), one can consider the Hugenholtz-Pines relation for the normal and anomalous self-energies $A(\omega,k)$, $B(\omega,k)$, respectively:

$$A(0,0)-B(0,0)=\mu. \quad (46)$$

The approximations in the previous section are equivalent to evaluating $A$ and $B$ at one-loop order. As explained by Popov,[42] this becomes

$$\mu=2g(\rho_0+\rho_1)-g(\rho_0+\tilde{\rho}_1)-2g^2\rho_0\sum_k[\mathcal{G}(k)\mathcal{G}(-k)-\mathcal{G}_1(k)\mathcal{G}_1(-k)]. \quad (47)$$

Here $\rho_0$ is the new condensate density, $\rho_1$ the density of noncondensed particles, and $\tilde{\rho}_1$ is an anomalous particle density, $\tilde{\rho}_1=\Sigma_k\mathcal{G}_1(k)$, with $\mathcal{G}_1$ the anomalous Green's function. The last term is a second-order correction due to the three boson vertices of the form $gA(a^\dagger a^\dagger a+a^\dagger aa)$. This last term in Eq. (47) can be evaluated to be $2g\tilde{\rho}_1$, leading to the result

$$\rho_0=\frac{\mu}{g}-(2\rho_1+\tilde{\rho}_1), \quad (48)$$

showing that $\rho_0+\rho_1$ is less than the saddle-point density.

Compare this expression for the total density to that from saddle point and fluctuations,

$$\rho=\rho_0+\rho_1=\rho_{\text{s.p.}}-\frac{\partial F_{\text{fluct}}}{\partial\mu}-\frac{d\psi_0}{d\mu}\frac{\partial F_{\text{fluct}}}{\partial\psi_0}, \quad (49)$$

where $\rho_{\text{s.p.}}=\mu/g$ is the saddle-point expectation of the density, and $F_{\text{fluct}}$ is the free energy from the fluctuation contributions. Since $\rho_1$, the density of noncondensed particles can be identified as

$$\rho_1=\sum_k\langle a_k^\dagger a_k\rangle=-\frac{\partial F_{\text{fluct}}}{\partial\mu}, \quad (50)$$

one must identify the depleted condensate density, Eq. (48) with

$$\rho_0=\frac{\mu}{g}-\frac{d\psi_0}{d\mu}\frac{\partial F_{\text{fluct}}}{\partial\psi_0}. \quad (51)$$

The derivatives with respect to the order parameter therefore describe a depletion of the order parameter due to fluctuations. Physically, interactions between the condensate and the finite population of noncondensed particles (at finite temperature) push up the chemical potential. With such a theory, there now exists a region of parameter space which is not condensed, but $\mu>0$. In such a region it is essential to include modifications of the particle spectrum due to interactions to describe the normal state.

*Comparison of methods* The phase boundary for the WIDBG model with static interactions is peculiarly insensitive to the calculation scheme. This can be seen by considering the Hugenholtz-Pines relation at the transition. In general, the anomalous self-energy vanishes at the transition, so $\mu=A(0,0)$. Since $\rho_0=0$, the total density is $\rho_1$, which may be found from the fluctuation Green's function, $\rho=\Sigma_{\omega,k}\mathcal{G}(\omega,k)$,

$$\mathcal{G}(\omega,k)=[i\omega+\epsilon_k-A(0,0)+A(\omega,k)]^{-1}, \quad (52)$$

where $\mu=A(0,0)$ has been used. If the self-energy is static, $A(\omega,k)=A(0,0)$, then at the transition the quasiparticles are exactly free. Any approximation scheme which gives $B(0,0)=0$ when $\rho_0=0$ will then reproduce this result. For this reason, partial derivatives will give correct calculations of the phase boundary for a dilute Bose gas, but this does not

remain true for dynamic self-energies.

For a boson-fermion model, such as polaritons, because of the dynamic self-energy, total and partial derivatives will give different answers. For the three-dimensional case studied by Ohashi and Griffin, this will lead to critical temperatures differing by a numerical factor, but in two dimensions using partial derivatives gives divergent answers. Were one to use partial derivatives, the density calculated from the condensed and noncondensed phases would agree at the critical chemical potential. However, for the total derivative, the density calculated at the new critical potential need not agree with that calculated from the noncondensed phase. A difference between these results reflects the fact that both are approximations of the phase boundary, and is indicative of the Ginzburg criterion.

### B. Total density for condensed polaritons

From the effective action, Eq. (12), the free energy per unit area, including quadratic fluctuations may be written as

$$\frac{F}{A} = \frac{S[\psi_0]}{A} + \frac{1}{\beta}\int_0^\infty \frac{d^2k}{(2\pi)^2}\sum_\omega \ln[|i\omega + \hbar\omega_k + K_1(\omega)|^2 - |K_2(\omega)|^2] = \left\{\hbar\tilde{\omega}_k\frac{|\psi_0|^2}{A} - \frac{\mu n}{2} - \frac{n}{\beta}\ln[\cosh(\beta E)]\right\} + \left\{\frac{1}{\beta}\int_0^\infty \frac{d^2k}{(2\pi)^2}\ln[1-e^{-\beta\hbar\tilde{\omega}_k}]\right\} \tag{53}$$

$$+ \frac{1}{\beta}\int_0^{K_m}\frac{d^2k}{(2\pi)^2}\left\{\ln\left[\frac{\sinh(\beta\xi_1/2)\sinh(\beta\xi_2/2)}{\sinh(\beta E)\sinh(\beta\hbar\tilde{\omega}_k/2)}\right] + \frac{1}{2}\ln\left[1 - \frac{\alpha 4E^2}{2(\hbar\tilde{\omega}_k E^2 - \hbar\tilde{\omega}_0\tilde{\epsilon}^2)}\right]\right\}. \tag{54}$$

Here $E$, $\alpha$, and $\xi_{1,2}$ are defined as in Sec. III. The first term in braces is $S[\psi_0]$, the second and third together are the fluctuation corrections. As discussed in Sec. II A, the interaction has been cut off at a scale $K_m$, so for $k > K_m$, the action is that of a free gas of photons, i.e., the second term in braces. In the third term, there are contributions both due to the Matsubara sum of Eq. (17), and due to the $\delta_\omega$ terms in Eq. (12), as discussed further in the Appendix, Sec. II.

The total density is then given by

$$\rho = \frac{|\psi_0|^2}{A} + \frac{n}{2}\left[1 - \frac{\tilde{\epsilon}}{E}\tanh(\beta E)\right] + \int_0^{K_m}\frac{d^2k}{(2\pi)^2}\left\{f[\xi_1] + f[\xi_2] - f[2E] + \frac{1}{2} + g(k)\right\} + \int_{K_m}^\infty \frac{d^2k}{(2\pi)^2}n_B(\hbar\tilde{\omega}_k), \tag{55}$$

where

$$f[x] = \left(n_B(x) + \frac{1}{2}\right)\left(-\frac{dx}{d\mu}\right),$$

$$g(k) = -\frac{1}{2\beta}\frac{1}{(1-C)}\frac{dC}{d\mu},$$

$$C = \frac{\beta\,\mathrm{sech}^2(\beta E)g^2 n}{2(\hbar\tilde{\omega}_k E^2 - \hbar\tilde{\omega}_0\tilde{\epsilon}^2)}\frac{g^2|\psi_0|^2}{A}.$$

In going from Eq. (54) and (55) the two integrals have been re-arranged, the second now describing only the free, high-energy photons. Again, the last term, $g(k)$, arises due to the $\delta_\omega$ terms.

The derivatives of polariton energies that arise in calculating the density may be given in terms of the expressions $A(k)$, $B(k)$ as defined in Eq. (18):

$$\frac{2\xi_{1,2}}{d\mu} = \frac{1}{4\xi_{1,2}}\left[\frac{dA(k)}{d\mu} \pm \frac{1}{\sqrt{A(k)^2 - B(k)}} \times \left(2A(k)\frac{dA(k)}{d\mu} - \frac{dB(k)}{d\mu}\right)\right], \tag{56}$$

$$\frac{dA(k)}{d\mu} = 8E\frac{dE}{d\mu} - 2\hbar\omega_k - 4\tilde{\epsilon} - 2\hbar\tilde{\omega}_0, \tag{57}$$

$$\frac{dB(k)}{d\mu} = 16\frac{\hbar^2k^2}{2m}\left(2E\frac{dE}{d\mu}\hbar\tilde{\omega}_k - E^2 + \tilde{\epsilon}\hbar\tilde{\omega}_0 + \tilde{\epsilon}^2\right). \tag{58}$$

To find $dE/d\mu$ in the presence of a condensate, one can differentiate the gap equation, Eq. (6), giving

$$-1 = \frac{dE}{d\mu}\frac{g^2 n}{2E^2}[\beta E\,\mathrm{sech}^2(\beta E) - \tanh(\beta E)]. \tag{59}$$

### C. Two dimensions, superfluid response

Having found an expression for the total density including fluctuations, it is necessary to consider how fluctuations change the critical chemical potential. As discussed in the introduction to this section, in two dimensions this requires consideration of the Kosterlitz-Thouless phase transition. The phase boundary is approximated from the condensed state by the chemical potential at which the superfluid response vanishes. We therefore must calculate the normal and superfluid response in the presence of a condensate.

#### *1. Calculating normal response density*

Following the standard procedure,[44,45] we consider the current,

$$\mathbf{J}(\mathbf{q},0) = \sum_{\mathbf{k},\omega}\frac{\hbar\mathbf{k}}{m}\psi^\dagger_{\mathbf{k}-\mathbf{q}/2}\psi_{\mathbf{k}+\mathbf{q}/2}. \tag{60}$$

For a perturbation $\delta H = \hbar\,\delta\mathbf{l}\cdot\mathbf{J}$, the linear response may be written $\langle J_i(q,0)\rangle = \chi_{ij}(q)\,\delta l_j(q)$. By symmetry, the most general response function is

$$\chi_{ij}(\mathbf{q}) = \chi_L(\mathbf{q})\frac{q_i q_j}{q^2} + \chi_T(\mathbf{q})\left(\delta_{ij} - \frac{q_i q_j}{q^2}\right). \tag{61}$$

By gauge symmetry, Eq. (60) is a conserved current. It follows, via a Ward identity, that $q_i\chi_{ij}(q) = q_j\,\mathrm{Tr}[\mathcal{G}(k)]$, so the total density is $\rho = m\chi_L(\mathbf{q}\to 0)/A$. In contrast, the transverse

response depends on only the density of normal particles, $\rho_{\text{normal}}=m\chi_T(\mathbf{q}\to 0)/A$.

In order to calculate the total density correctly, it is necessary to introduce vertex corrections, i.e.,

$$\chi_{ij}(\mathbf{q}\to 0)=\mathrm{Tr}(\Gamma_i(\mathbf{k},\mathbf{k})\mathcal{G}(\mathbf{k})\gamma_j(\mathbf{k},\mathbf{k})\mathcal{G}(\mathbf{k})), \tag{62}$$

where $\gamma_i(\mathbf{p},\mathbf{q})=\sigma_3(p_i+q_i)/2m$, and $\Gamma_i(p,q)$ is chosen to satisfy the Ward identity. However, the diagrams required to satisfy the Ward identity (see Ref. 44) take the form

$$\Gamma_i(\mathbf{p},\mathbf{q})=\gamma_i(\mathbf{p},\mathbf{q})+(p_i-q_i)f(p,q). \tag{63}$$

This form of the vertex correction means only the longitudinal response is affected. Therefore the standard procedure is to calculate the total density directly from the free energy, as in Sec. IV B, and the normal density by linear response.

To one-loop order, and neglecting vertex corrections, the response function is given by

$$\chi_{ij}(\mathbf{q}\to 0)=\frac{1}{\beta}\sum_{\mathbf{k},\omega}\frac{\hbar^2k_ik_j}{m^2}\mathrm{Tr}[\mathcal{G}(\mathbf{k})\sigma_3\mathcal{G}(\mathbf{k})\sigma_3], \tag{64}$$

and so, taking the continuum limit, the normal density is given by

$$\rho_n=\int_0^\infty\frac{d^2k}{(2\pi)^2}\frac{\hbar^2k^2}{2m}\frac{1}{\beta}\sum_\omega\mathrm{Tr}[\mathcal{G}(\mathbf{k})\sigma_3\mathcal{G}(\mathbf{k})\sigma_3]. \tag{65}$$

For the polariton system, the trace can be evaluated to give

$$\rho_{\mathrm{n}}=\int_0^\infty\frac{d^2k}{(2\pi)^2}\frac{\hbar^2k^2}{2m}\frac{1}{\beta}\sum_\omega\frac{[i\omega+\hbar\tilde{\omega}_k+K_1(\omega)]^2+[-i\omega+\hbar\tilde{\omega}_k+K_1^*(\omega)]^2-2|K_2(\omega)|^2}{[|i\omega+\hbar\tilde{\omega}_k+K_1(\omega)|^2-|K_2(\omega)|^2]^2} \tag{66}$$

$$=\int_0^\infty\frac{d^2k}{(2\pi)^2}\frac{\hbar^2k^2}{2m}\frac{1}{\beta}\left\{\sum_\omega\frac{[2\tilde{\omega}_0(i\tilde{\epsilon}\omega-E^2-\tilde{\epsilon}^2)+(i\omega+\tilde{\omega}_k)(\omega^2+4E^2)]^2-[2\tilde{\omega}_0(E^2-\tilde{\epsilon}^2)]^2}{(\omega^2+\xi_1^2)^2(\omega^2+\xi_2^2)^2}+\mathrm{C}_0(k)\right\}. \tag{67}$$

Again, in evaluating the Matsubara sum, one must consider the $\delta_\omega$ terms. The term $C_0(k)$ is the difference between the true term at $\omega=0$, and the analytic continuation appearing in the Matsubara sum in Eq. (67), and is given by

$$\mathrm{C}_0(k)=2\alpha\times\left[\left(\frac{\hbar^2k^2}{2m}\right)\left(\frac{\hbar^2k^2}{2m}+\frac{g^2|\psi_0|^2}{A}\frac{\hbar\tilde{\omega}_0}{E^2}\right)\left(\frac{\hbar^2k^2}{2m}+\frac{g^2|\psi_0|^2}{A}\frac{\hbar\tilde{\omega}_0}{E^2}-2\alpha\right)\right]^{-1}, \tag{68}$$

with $\alpha$ as defined in Eq. (15).

#### 2. Total photon density

For the polariton system there is an added complication. Equation (67) gives the density of normal photons, but Eq. (55) is the total excitation density (including excitons). It is therefore necessary to calculate the total photon density.

This can be done by considering separate chemical potentials for photons and excitons, which are set equal at the end of the calculation. This means making the change,

$$\mu N\to\mu_{\mathrm{ex.}}\sum_{j=1}^{j=nA}\left(S_j^z+\frac{1}{2}\right)+\mu_{\mathrm{phot.}}\sum_k\psi_k^\dagger\psi_k, \tag{69}$$

in the action. The photon density is then total derivative with respect to the photon chemical potential $\mu_{\mathrm{phot}}$.

This density is given by Eq. (55) with two changes. First, the mean-field exciton density,

$$\frac{n}{2}\left[1-\frac{\tilde{\epsilon}}{E}\tanh(\beta E)\right], \tag{70}$$

should be removed. Second, in $f[x],g(k)$ derivatives should be taken with respect to $\mu_{\mathrm{phot}}$. This means replacing Eqs. (57) and (58) by

$$\frac{dA(k)}{d\mu_{\mathrm{phot.}}}=8E\frac{dE}{d\mu}-2\hbar\omega_k-4\tilde{\epsilon}, \tag{71}$$

$$\frac{dB(k)}{d\mu_{\mathrm{phot.}}}=16\frac{\hbar^2k^2}{2m}\left(2E\frac{dE}{d\mu}\tilde{\omega}_k-E^2+\tilde{\epsilon}^2\right). \tag{72}$$

This makes use of the fact that $dE/d\mu_{\mathrm{phot}}=dE/d\mu$, as can be seen from the gap equation.

## V. PHASE BOUNDARY INCLUDING FLUCTUATIONS

Combining the results of Sec. IV, the phase boundary is found by plotting the total density [Eq. (55)] at the value of chemical potential where the normal photon density [Eq. (67)] matches the total photon density (discussed in Sec. IV C 2). The phase boundaries found in this way are plotted in Fig. 4. The form of the phase boundary can be explained by considering how, at finite temperatures, the occupation of excited states of the system depletes the condensate. Which excited states are relevant changes with density.

### A. Resonant case

When condensed, the lowest energy mode is the phase mode, described by Eq. (23). At low density, this has a shal-

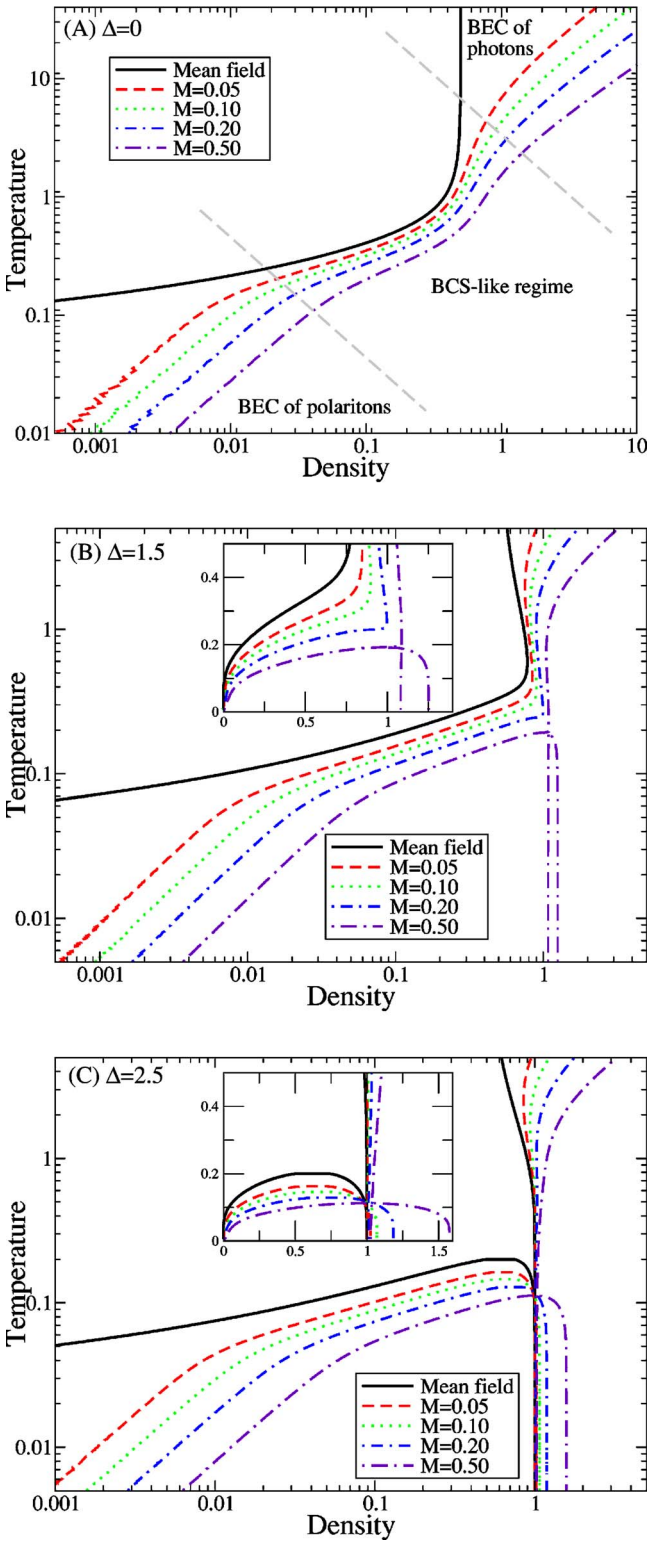


FIG. 4. (Color online) Mean-field phase boundary, and phase boundaries including fluctuation correction for four values of photon mass, on a logarithmic scale (Insets are on a linear scale). Panel (A) is the resonant case, $\Delta=0$, adapted from Ref. 15 and shown for comparison. In panels (B) and (C), the exciton is detuned below the photon band by $\Delta=1.5g\sqrt{n}$ and $\Delta=2.5g\sqrt{n}$, respectively. Temperature plotted in units of $g\sqrt{n}$ and density in units of $n$.

low slope, and consequently a large density of states. Such excitations are described in a model of point bosons. The phase boundary can therefore be estimated from the degeneracy temperature of a gas of polaritons, of mass $2m$, where $m$ is the bare photon mass:

$$k_B T_{deg} = \frac{2\pi\hbar^2}{2(2m)}\rho = g\sqrt{n}\frac{\pi}{2m^*}\frac{\rho}{n}. \tag{73}$$

As the density increases, the phase mode becomes steeper, and so has a smaller density of states. The relevant excitations are then single-particle excitations across the gap. Such excitations are accounted for in the mean-field theory. Combining Eqs. (6) and (7) gives the result

$$k_B T_c = g\sqrt{n}\frac{\sqrt{1-2\rho/n}}{2\tanh^{-1}(1-2\rho/n)} \approx \frac{g\sqrt{n}}{-\ln(\rho/n)}. \tag{74}$$

As seen in Fig. 4, the mean-field boundary is effectively constant on the scale of the boundary for BEC of point bosons, and so the crossover to mean field always occurs near $k_B T \approx g\sqrt{n}$, the Rabi splitting. The density at which this crossover occurs depends on the photon mass. Comparing Eqs. (73) and (74), this crossover occurs at a density $\rho_{\text{crossover}} \approx nm^*$.

In terms of the measurable Rabi splitting, $g\sqrt{n}$, and polariton mass $m$, this gives the density

$$\rho_{\text{crossover}} = \frac{mg\sqrt{n}}{\hbar^2}. \tag{75}$$

For the structures studied by Yamamoto *et al.*,[2–4] $g\sqrt{n} \approx 7$ meV and $m \approx 10^{-5} m_{\text{electron}}$. These values give a crossover density of $\rho_{\text{crossover}} = 2.6\times10^8$ cm$^{-2}$. This is both much less than the estimates of experimentally achieved density, $n \sim 10^{11}$ cm$^{-2}$ per pulse, and also much less than the Mott density in this structure, $n_{\text{Mott}} \approx 3.6\times10^{13}$ cm$^{-2}$. For the structures studied by Dang *et al.*,[1,5] $g\sqrt{n} \approx 13$ meV, and $m \approx 3\times10^{-5} m_{\text{electron}}$, so crossover densities are again of the same order, $\rho_{\text{crossover}} = 5\times10^8$ cm$^{-2}$. Dang *et al.* also present results for the detuned case,[5] discussed below, with a range of dimensionless detunings $0.5 > \Delta^* > -0.7$.

Equation (75) describes the crossover in terms of properties measurable for a given microcavity. However, to understand what fundamental length scales control this crossover density, it is necessary to write the coupling strength and polariton mass in terms of the dimensions of the cavity and properties of the excitons. Using the expressions in Sec. II for photon mass and coupling strength $g$, this gives the crossover density as

$$\rho_{\text{crossover}} = 4\pi^2\sqrt{\frac{e^2}{4\pi\varepsilon_0\hbar c}}\frac{1}{\varepsilon_r^{1/4}}\frac{d_{ab}\sqrt{n}}{w^2}. \tag{76}$$

The crossover density is therefore controlled by two parameters: The width of the cavity $w$ and the ratio of electron-hole separation to average two-level system separation, $d_{ab}\sqrt{n} = d_{ab}/r_{\text{separation}}$. If the average two-level system separation ($r_{\text{separation}}$) is less than the electron-hole separation ($d_{ab}$), then our model of localized two-level systems will break down. Therefore within our model the largest possible cross-

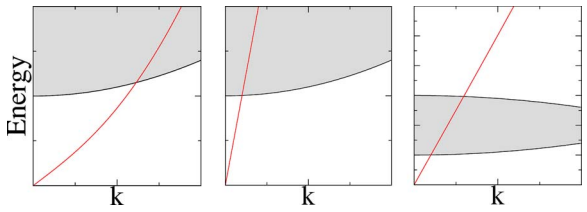


FIG. 5. (Color online) A schematic picture of how the relevant excitations change between the polariton BEC, the BCS-like mean-field, and the photon BEC regimes. In the low-density limit, a shallow sound mode exists. At higher densities, this becomes steeper, and the relevant excitations are gapped single-particle excitations. At yet higher densities, these modes are saturated, and the high $k$ photon modes become relevant.

over density scale is $1/w^2$. This length scale occurs because the cavity size controls the wavelength of the lowest radiation mode. Crossover to a BCS-like mean-field regime occurs when the density approaches a scale set by the wavelength of light, rather than one set by the exciton Bohr radius. Therefore in general this crossover density is much less than the Mott density.

At yet higher densities, the single-particle excitations are saturated, and so the condensate becomes photon dominated. In this regime, the transition temperature is that for a gas of massive photons. If the photon mass is large ($m^* > 1$), a mean-field regime never exists, instead the phase boundary changes directly from polariton condensation to a photon condensation. However, since for experimental parameters the dimensionless mass is only of the order of $10^{-3}$, a mean-field regime will exist. These various crossovers are illustrated schematically in Fig. 5.

### B. Effects of detuning

If the excitons are detuned below the photon (positive detuning), it becomes possible for the system to reach half filling while remaining uncondensed. For positive detunings greater than $2g\sqrt{n}$ the mean-field phase boundary becomes re-entrant, as shown in the bottom panel of Fig. 4. For smaller but still positive detunings, the mean-field boundary has a maximum critical density at a finite temperature, but no maximum of critical temperature. The opposite case, of excitons detuned above photons, shows no interesting features; the system will always condensed before half filling.

This multivalued phase boundary is discussed in Ref. 14, and can be explained in terms of phase locking of precessing spins,[46] either about spin-down (low density) or spin-up (high density) states. Above inversion, increasing the density reduces the extent to which a spin may precess. For very large detunings, at low temperatures, the phase diagram therefore becomes symmetric about half filling.

When $\Delta \geqslant 2g\sqrt{n}$, the re-entrance leads to a point at zero temperature where two second-order phase boundaries meet. Including fluctuations, as shown in the bottom panel of Fig. 4, these phase boundaries no longer meet, but instead there is a region where two different condensed solutions coexist. In this region, there are two minima of the free energy, so we expect there will be a first-order phase boundary between

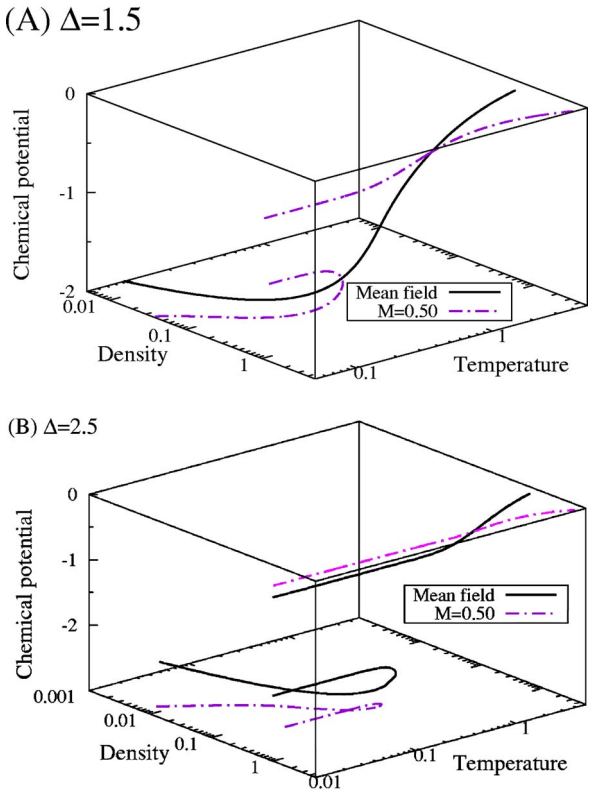


FIG. 6. (Color online) Chemical potential vs density and temperature at the phase boundary, for the mean-field phase boundary, and $m^*=0.50$ fluctuation corrections. Plotted for detunings of $\Delta = 1.5g\sqrt{n}$ [panel (A)] and $\Delta = 2.5g\sqrt{n}$ [panel (B)], with all other parameters as in Fig. 4. Temperature and chemical potential plotted in units of $g\sqrt{n}$, and density in units of $n$.

them. Although this boundary could be calculated by comparing the free energies including fluctuations, its form may be altered significantly by higher-order corrections.

In the mean-field theory, at zero temperature, the chemical potential jumps discontinuously at the point where the two phase boundaries meet. This can be understood by the chemical potential locking to the lower polariton for the lower density transitions, and to the upper polariton at higher densities. This can be seen in the lower panel of Fig. 6, which plots the value of the chemical potential at the phase boundary. Including fluctuations, the jump in chemical potential has a similar form, and is somewhat larger. In the region of coexistence discussed above, the two minima of free energy have different chemical potentials, so at the first-order transition, the chemical potential will jump.

At smaller detunings, as shown in the central panel of Fig. 4, although the mean-field phase boundary is single valued, adding fluctuations can reproduce the same coexistence regions. For this to occur, the photon mass must be large—i.e., there must be a significant density of states for fluctuations. As shown in the upper panel of Fig. 6, this coexistence is also characterized by two minima of the free energy, with different chemical potentials, and so is also expected to become a first-order transition in the same manner.

To explain how fluctuations lead to the introduction of multiple phase boundaries at a single temperature, it is nec-

essary to consider the upper branch of excitations, $\xi_2(k)$. With positive detuning, the energy of this mode (with respect to chemical potential) can continue to fall as the chemical potential increases in the condensed state. This has two effects, it makes the sound velocity larger [as can be seen from Eq. (23)], and increases the population of this "pair-breaking" upper mode. The combination of these effects is responsible for the creation of the coexistence region by fluctuations.

### C. Effects of inhomogeneous broadening

It is interesting to consider how a small inhomogeneous broadening will modify the phase boundary. Exact calculations with a continuum of exciton energies are technically challenging and not particularly illuminating, so the following presents a discussion of the main effects expected. The following discussion is for a Gaussian distribution of energies, centered at the bottom of the photon band, with a standard deviation much less than $g\sqrt{n}$.

The most significant change to the boundary is due to the existence of a low-energy tail of excitons. This means that, even at low densities, the chemical potential lies within the exciton band, and a BCS-like form of $T_c$ will be recovered. Consider the density of states,

$$\nu_s(\epsilon) = \frac{\exp(-\epsilon^2/2\sigma^2)}{\sqrt{2\pi}\sigma}. \tag{77}$$

For large negative chemical potentials, at low temperatures and densities, the saddle-point equation (6) becomes

$$\frac{\hbar\omega_0}{g^2} = \frac{1}{g_{\text{eff}}} = \int_{-\infty}^{\infty} \frac{\tanh(\beta\tilde{\epsilon})}{2\tilde{\epsilon}} \nu_s(\epsilon) d\epsilon,$$

$$\approx \nu_s\left(\frac{\mu}{2}\right)\left[1 + \ln\left(\frac{\Lambda}{T}\right)\right], \tag{78}$$

and the mean-field density (7), using the asymptotic form of the error function, is

$$\rho_{\text{M.F.}} = \nu_s\left(\frac{\mu}{2}\right)\left(\frac{\sigma^2}{-\mu}\right). \tag{79}$$

The cutoff $\Lambda$ is approximately $2\sigma^2/\mu$, but appears only as a pre-exponential factor, and so the density dependence it gives to $T_c$ will be neglected. Thus the mean-field transition temperature at low densities then becomes

$$k_B T_c = \Lambda \exp\left(-\frac{2\sigma^2}{g^2\rho}\right). \tag{80}$$

For low densities, this result is very different to the mean-field theory without broadening, Eq. (74). Whereas before the mean-field boundary was approximately constant, it now drops rapidly to zero. If one now considers how fluctuations will modify this boundary, it is more helpful to consider the density as a function of temperature. At low temperatures, fluctuations increase the density by a small amount, $\Delta\rho \propto T$. Without broadening, the mean-field critical density is approximately $\rho \approx n e^{-g\sqrt{n}/T}$ and goes to 0 faster than the fluctuation corrections, $\Delta\rho$. Therefore as shown in Fig. 4, at low temperatures the fluctuation contribution controls the phase boundary. With broadening the mean-field critical density at low temperature is approximately $\rho \approx 2\sigma^2/g^2 \ln(\Lambda/T)$, which goes to zero more slowly than $\Delta\rho$. Therefore including fluctuations in this regime does not change the form of the phase boundary drastically. Hence at very low densities, the boundary is again well described by a mean-field theory.

### D. Relation to alternate models and experimental systems

Our model describes two-level systems with a finite total density of states—the density of states, per unit area, integrated over all energies, is finite. As will be explained below, this finite total density of states is responsible for the re-entrant behavior seen in the mean-field theory for detunings $\Delta \geqslant 2g\sqrt{n}$. In the preceding sections, the finite total density of states has also been implicated in explaining the existence of a photon dominated region at high temperature, and the multivalued phase boundary in the presence of fluctuations. This section discusses how these effects may change in alternate models which do not have saturable two-level systems. Although the multivalued phase boundary is expected only to occur for a finite band of two-level systems, the existence of a photon dominated regime at high densities is more general.

Before discussing the more involved question of how changing the density of states affects fluctuations, we first summarize its effect on the mean-field theory.[14,16,47] Consider the highest possible density achievable in the normal state. Since there exists a Bosonic mode, the chemical potential cannot exceed the energy of this mode if the system is to remain normal. Therefore at zero temperature, only exciton modes below the boson mode are relevant. Regardless of whether the total density of states is finite, the density of states below the Bosonic mode will be finite. However, at nonzero temperatures, exciton modes above the chemical potential can be occupied by the tail of the Fermi distribution. If there is a finite total density of states, there will be a maximum density of excitons that can be occupied thermally. This is what is referred to as "saturation" below. Note that for a exciton band centered at the bottom of the photon band, this maximum density of excitons is half the density of two-level systems—the system saturates at half filling. If the total density of states is not finite, it is possible to support any total density in the normal state by making the temperature high enough.

This saturation is responsible for the multivalued phase boundary in the mean-field theory. If the density is close to total inversion of the two-level systems, all two-level systems must be in the up state. This makes it hard for them to produce a macroscopic polarisation—viewed as spins, this is to say that if $S_z \approx +1/2$, then $S_x$ will be small. Hence the system becomes uncondensed near total inversion. If the excitation density is greater than the density of two-level systems, the mean-field theory requires a coherent photon density. Hence the system condenses again, giving a re-entrant boundary. Without saturable excitons, neither the uncondensing due to reduction of mean-field polarization, or the recondensation due to exciton saturation will occur. With fluc-

tuations, the multivalued phase boundary is analogous to the mean-field re-entrance, and appears to require saturable excitations in the same manner. Therefore we do not expect such multivalued phase boundaries in a general model with a continuum of exciton states.

Let us now consider the case where there is a finite density of exciton states, separated by the exciton binding energy from a continuum of electron-hole states. In such a case, if the continuum is well separated from bound states, it may only affect the phase boundary at densities larger than those where the features discussed above occur. Well separated here means that the exciton binding energy is much larger than the energy scales in our model, in particular, much larger than $g\sqrt{n}$. If the continuum only has effects at very high densities, the exotic multivalued phase boundary described in previous sections will be realizable. For the systems studied by Yamamoto *et al.*,[3] $g\sqrt{n} \approx 7$ meV, and the exciton binding energy $Ryd^* \approx 10$ meV. For Dang *et al.*,[1] $g\sqrt{n} \approx 13$ meV, and $Ryd^* \approx 25$ meV. In neither case can the effects of the continuum be avoided. Reducing the Rabi splitting, $g\sqrt{n}$, might allow the multivalued phase boundary to be observed. However, reducing the Rabi splitting will decrease the transition temperature in the region of interest. In addition, to have strong coupling, the Rabi splitting must remain larger than the polariton linewidth due to photon lifetimes.

The existence of a photon dominated region at high densities is, however, generic, and does not rely on a model with a finite total density of states. In an electron-hole plasma model,[37,48] such a regime is also predicted. At large densities, as the chemical potential (lying within the exciton band) approaches the bottom of the photon band, the photon density increases much faster than the exciton density. The result in Ref. 37 only describes a photon dominated regime at zero temperature. For the two-level system model, at high densities, the system remains photon dominated, and with increasing temperature changes from coherent to incoherent photons. Such a change from coherent to incoherent photons is also expected to occur in the electron-hole model, due to the large occupation of Bosonic modes near the chemical potential, but further work is required here.

This discussion of how our model relates to experimental systems has so far concentrated on what happens at high densities. At lower densities (including the densities of current experiments), no such significant differences are expected. This is because, at low densities, higher energy exciton modes would not be occupied, even if they exist. In particular, the angular distribution of radiation (Fig. 3) and excitation spectrum (Figs. 1 and 2) should remain unchanged for generic models. Such signatures should therefore be expected for equilibrium condensation in the systems currently studied.

The signatures of condensation presented in this paper are calculated for a system in thermal equilibrium, while current experiments are pumped. For nonresonantly pumped experiments,[1–5] one must consider how pumping will modify the excitation spectrum and the occupation of modes. This can be described by coupling the system to baths describing pumping of excitons and decay of photons. For systems near equilibrium, with small coupling to baths, one expects the excitation spectrum to remain close to the equilibrium case, but with nonthermal occupations. Even with nonthermal occupation, the large density of states for excitations near the chemical potential can be expected to produce a peak in the angular distribution of radiation. For strong coupling to baths, the spectrum of excitations will also change. One particularly significant change is the possibility of giving a finite lifetime to the Goldstone mode. In this strongly pumped region, the signatures predicted in this paper can be expected to change significantly.

It is also of interest to discuss how these signatures are related to the behavior seen in resonantly pumped cavities.[8–10] In these experiments pumping at a critical angle excites polaritons at momentum $k_p$, causing emission from signal, $k=0$, and idler, $k=2k_p$, modes. Such a system may be described as an optical parametric oscillator. Above a threshold, the luminescence from the signal increases superlinearly, and the signal linewidth narrows dramatically. In such a system, the occupation of the signal mode obeys a self-consistency condition, and the relative phase between the pump and signal mode is free. However, the nature of this self-consistency differs from that for an equilibrium condensate, and thus the signatures of equilibrium condensation are no longer immediately applicable.

The form of the condensed luminescence spectrum, and the angular distribution of polaritons depend on the existence of the low-energy Goldstone mode. The energy of this mode vanishes as $k \to 0$ as a consequence of the gap equation, Eq. (6), which means that global phase rotations cost no energy. In a laser, the coherent field is also set by a self-consistency condition, balancing pumping and decay. Like condensation, the laser transition can also be described as symmetry breaking.[49] However, because the self-consistency relates imaginary parts of the self-energy, the dynamics of modes near the lasing mode is diffusive. Therefore a free global phase and a self-consistency condition are not sufficient for the signatures described in this paper.

For the optical parametric oscillator experiments, the self-consistency equation is complicated by the existence of a coherent idler field.[50,51] Since such experiments are strongly pumped it is expected that, despite the free phase and self-consistency, the luminescence spectrum and angular distribution of radiation as described in this paper will not be applicable. The laser and the equilibrium condensate are extreme cases, and the distinction in practice is less clear.[10,46] For example, adding decoherence[52,53] to an equilibrium condensate causes a crossover to a regime better described as a laser.

## VI. CONCLUSIONS

We have studied the effect of fluctuations about the mean-field theory for a model of localized excitons coupled to a continuum of photon modes. When condensed, the presence of a gap in the fermion density of states, and the existence of the phase mode, cause dramatic changes to the spectrum of collective modes. Such changes lead to signatures of condensation in the luminescence and absorption spectrum (Fig. 2), and in the momentum distribution of radiation escaping the cavity (Fig. 3).

Including the contribution to density due to fluctuations, we have studied the crossover from a BEC of polaritons at low densities, through a BCS-like mean-field regime at intermediate densities, and finally to a BEC of massive photons at high densities, as shown in Fig. 4. The BCS-like regime occurs at densities achieved in current experiments. Our study of the crossover can be compared to other studies of the crossover; in Feshbach resonance systems,[27,54] or for fermions interacting via a static four-particle interaction.[33,40] In distinction to those systems, due to the nature of the fermion density of states in our system, there is no clear difference between the rôles of the number and gap equations in the BEC- and BCS-like regimes. Rather, the crossover is in the nature of the fluctuations that depopulate the condensate.

At low densities, fluctuation corrections significantly alter the form of the phase boundary from its mean-field form, leading to a dependence $T \propto \rho$. As the density increases, the transition temperature approaches the Rabi splitting, and those single-particle excitations which are included in the mean-field calculation dominate, leading to a recovery of the mean-field limit. This occurs at a density scale set by the wavelength of light, not the exciton separation, and so at densities much less than the Mott density. At yet higher densities, the system becomes photon dominated and the boundary is that for a BEC of massive photons. If the exciton is detuned below the photon, the mean-field boundary can become multivalued. With fluctuations, this multivalued structure occurs for smaller detunings than are required for it to occur in the mean-field theory. At least for a saturable two-level systems, this multivalued boundary likely indicates a first-order transition between two condensed states.

Because our system is two dimensional, it required fluctuations to be considered in the presence of the condensate. In the presence of a condensate it is important to consider changes to the density both due to "condensate depletion" as well as the occupation of fluctuation modes. Such condensate depletion is included by taking full derivatives of the action with respect to the chemical potential.

## ACKNOWLEDGMENTS

We are grateful to H. Deng, L. S. Dang, F. M. Marchetti, B. D. Simons, and Y. Yamamoto for useful discussions. We acknowledge financial support from the Cambridge-MIT Institute (J.K.), Sidney Sussex college, Cambridge (P.R.E.), Gonville and Caius College Cambridge (M.H.S.), and the EU Network "Photon mediated phenomena in semiconductor nanostructures," HPRN-CT-2002-00298.

## APPENDIX: LEHMANN REPRESENTATION AND BROKEN SYMMETRY

### 1. Analytic properties of thermal and retarded Green's functions

The inverse thermal Green's function contains terms proportional to $\delta_\omega$. Working from the Lehmann representation, it may be shown that such terms can arise in the thermodynamic Green's function, but not in the dynamic Green's functions.

To see this, consider the standard Lehmann representation (see, e.g., Ref. 55, Sec. 17) for the retarded Green's function for Bose fields:

$$G_{\mathrm{R}}(\omega) = \lim_{\delta \to 0^+} \int_{-\infty}^{\infty} \frac{\rho_L(x)dx}{x - (\omega + i\delta)}, \tag{A1}$$

$$\rho_L(x) = (1 - e^{-\beta x}) \sum_{n,m} |\langle n|\psi|m\rangle|^2 e^{\beta(F - E_n)} \delta(x - E_{mn}).$$

However, for the thermal Green's function, an extra term may appear,

$$\mathcal{G}(\omega) = \int_0^\beta d\tau e^{i\omega\tau} \mathrm{Tr}(e^{\beta(F-H)} e^{H\tau} \psi e^{-H\tau} \psi^\dagger)$$

$$= \sum_{n,m} |\langle n|\psi|m\rangle|^2 e^{\beta(F-E_n)} \int_0^\beta e^{(i\omega - E_{mn})\tau} d\tau \tag{A2}$$

$$= \int_{-\infty}^{\infty} \frac{\rho_L(x)dx}{x + i\omega} + \beta\delta_\omega \sum_{n,m} |\langle n|\psi|m\rangle|^2 e^{\beta(F-E_n)} \delta(E_{mn}). \tag{A3}$$

The last term in Eq. (A3) can be identified as the contribution to the Green's function due to transitions between degenerate states, or due to a macroscopic occupation of the photon in the ground state. Such a term does not occur for the retarded Green's function, and so in calculating the spectral Lehmann density $\rho_L(x)$, one may neglect its effects.

### 2. Matsubara summation with thermal Green's functions

The $\delta_\omega$ terms will contribute to Matsubara sums involving the thermal Green's functions, in properties such as the density. In performing the Matsubara summation one must use

$$\sum_{\omega_n} f(\omega_n) = \int_{-\infty}^{\infty} \frac{dz}{2\pi i} A(z) + f(0),$$

$$A(z) = \lim_{\delta \to 0} 2\,\mathrm{Im}\left[\tilde{f}(z') \frac{\beta}{2} \coth\left(\frac{\beta z'}{2}\right)\right]_{z' = z + i\delta}, \tag{A4}$$

where although $A(z)$ involves $\tilde{f}$, the analytic continuation of $f$, $f(0)$ does not involve analytic continuation. If the analytic continuation of $f$ is regular at $z=0$, then

$$\sum_{\omega_n} f(\omega_n) = \sum_{\text{poles of } f} \mathrm{res}\left[\tilde{f}(z) \frac{\beta}{2} \coth\left(\frac{\beta z}{2}\right)\right] + f(0) - \tilde{f}(0), \tag{A5}$$

i.e., one must add a term to correct for the difference between $f$ and its analytic continuation at $z=0$.

### 3. Emission and absorption coefficients

Considering the Green's function for photon fluctuations; at zero temperature the function $\rho_L(x)$ would give the density

of states, weighted by the photon component of a state. At finite temperatures, one may extract the probability to emit a photon,

$$P_{\text{emit}}(x) = \sum_{n,m} |\langle m|\psi|n\rangle|^2 e^{\beta(F-E_n)} \delta(x + E_{mn}) = n_{\text{B}}(x)\rho_L(x), \tag{A6}$$

or to absorb a photon,

$$P_{\text{absorb}}(x) = \sum_{n,m} |\langle m|\psi^\dagger|n\rangle|^2 e^{\beta(F-E_n)} \delta(x - E_{mn}) = (1 + n_{\text{B}}(x))\rho_L(x), \tag{A7}$$

The energy $x$ is measured with respect to the chemical potential, so at zero temperature there is only emission of photons at energies below the chemical potential, or absorption of photons above the chemical potential. The Lehmann density itself, $\rho_L(x)$, is the difference of these, and can be interpreted as an absorption coefficient which, when negative, represents gain.

*Electronic address: jmjk2@cam.ac.uk


[1] L. S. Dang, D. Heger, R. André, F. Bœuf, and R. Romestain, Phys. Rev. Lett. **81**, 3920 (1998).

[2] H. Deng, G. Weihs, C. Santori, J. Bloch, and Y. Yamamoto, Science **298**, 199 (2002).

[3] H. Deng, G. Weihs, D. Snoke, J. Bloch, and Y. Yamamoto, Proc. Natl. Acad. Sci. U.S.A. **100**, 15318 (2003).

[4] G. Weihs, H. Deng, D. Snoke, and Y. Yamamoto, Phys. Status Solidi A **201**, 625 (2004).

[5] M. Richard, J. Kasprzak, R. André, L. S. Dang, and R. Romenstain, J. Phys.: Condens. Matter **16**, S3683 (2004).

[6] A. Baas, J.-P. Karr, M. Romanelli, A. Bramati, and E. Giacobino, cond-mat/0501260.

[7] S. Savasta, O. D. Stefano, V. Savona, and W. Langbein, Phys. Rev. Lett. **94**, 246401 (2005) .

[8] J. J. Baumberg, P. G. Savvidis, P. G. Lagoudakis, M. D. Martin, D. Whittaker, R. Butte, M. Skolnick, and J. Roberts, Physica E (Amsterdam) **13**, 385 (2002).

[9] P. G. Savvidis, J. J. Baumberg, R. M. Stevenson, M. S. Skolnick, D. M. Whittaker, and J. S. Roberts, Phys. Rev. Lett. **84**, 1547 (2000).

[10] J. J. Baumberg, P. G. Savvidis, R. M. Stevenson, A. I. Tartakovskii, M. S. Skolnick, D. M. Whittaker, and J. S. Roberts, Phys. Rev. B **62**, R16247 (2000).

[11] A. Kavokin, G. Malpuech, and F. P. Laussy, Phys. Lett. A **306**, 187 (2003).

[12] F. P. Laussy, G. Malpuech, A. Kavokin, and P. Bigenwald, Phys. Rev. Lett. **93**, 016402 (2004).

[13] F. Tassone, C. Piermarocchi, V. Savona, A. Quattropani, and P. Schwendimann, Phys. Rev. B **56**, 7554 (1997).

[14] P. R. Eastham and P. B. Littlewood, Phys. Rev. B **64**, 235101 (2001).

[15] J. Keeling, P. R. Eastham, M. H. Szymanska, and P. B. Littlewood, Phys. Rev. Lett. **93**, 226403 (2004).

[16] P. R. Eastham and P. B. Littlewood, Solid State Commun. **116**, 357 (2000).

[17] D. G. Lidzey, D. D. C. Bradley, T. Virgili, A. Armitage, M. S. Skolnick, and S. Walker, Phys. Rev. Lett. **82**, 3316 (1999).

[18] D. G. Lidzey, D. D. C. Bradley, M. S. Skolnick, T. Virgli, S. Walker, and D. M. Whittaker, Nature (London) **395**, 53 (1998).

[19] U. Woggon, R. Wannemacher, M. V. Artemyev, B. Moller, N. Lethomas, V. Anikeyev, and O. Schops, Appl. Phys. B: Lasers Opt. **77**, 469 (2003).

[20] J. P. Reithmaler, G. Sęk, A. Löffer, C. Hoffmann, S. Kuhn, S. Reitzenstein, L. Keldysh, V. D. Kulakovskii, T. L. Reinecke, and A. Forchel, Nature (London) **432**, 197 (2004).

[21] T. Yoshi, A. Schere, J. Hendrickson, G. Khitrova, H. M. Gibbs, G. Rupper, C. Ell, O. B. Shchekin, and D. G. Deppe, Nature (London) **432**, 200 (2004).

[22] H. F. Hess, E. Betzig, T. D. Harris, L. N. Pfeiffer, and K. W. West, Science **264**, 1740 (1994).

[23] A. Pawlis, A. Kharchenko, O. Husberg, K. Lischka, and D. Schikora, J. Phys.: Condens. Matter **16**, S3689 (2004).

[24] T. Tawara, H. Gotoh, T. Akasaka, N. Kobayashi, and T. Saitoh, Phys. Rev. Lett. **92**, 256402 (2004).

[25] M. Holland, S. J. J. M. F. Kokkelmans, M. L. Chiofalo, and R. Walser, Phys. Rev. Lett. **87**, 120406 (2001).

[26] E. Timmermans, P. Tommasini, M. Hussein, and A. K. Kerman, Phys. Rep. **315**, 199 (1999).

[27] Y. Ohashi and A. Griffin, Phys. Rev. A **67**, 063612 (2003); but see cond-mat/0302196 for expanded version.

[28] R. H. Dicke, Phys. Rev. **93**, 99 (1954).

[29] K. Hepp and E. Lieb, Phys. Rev. A **8**, 2517 (1973).

[30] K. Rzążewski, K. Wódkiewicz, and W. Żakowicz, Phys. Rev. Lett. **35**, 432 (1975).

[31] V. Popov and S. Fedotov, Sov. Phys. JETP **67**, 535 (1988); [Zh. Eksp. Teor. Fiz. **94**, 183 (1988)].

[32] J. R. Schrieffer, *Theory of Superconductivity* (Perseus Books, Reading, Massachusetts, 1999).

[33] M. Randeria, in *Bose-Einstein Condensation*, edited by A. Griffin, D. Snoke, and S. Stringari (Cambridge University Press, Cambridge, UK, 1995), p. 355.

[34] Y. Ohashi and S. Takada, J. Phys. Soc. Jpn. **66**, 2437 (1997).

[35] S. T. Beliaev, Sov. Phys. JETP **7**, 299 (1958) [J. Exp. Theor. Phys. **34**, 433 (1958).

[36] J. Keeling, L. S. Levitov, and P. B. Littlewood, Phys. Rev. Lett. **92**, 176402 (2004).

[37] F. M. Marchetti, B. D. Simons, and P. B. Littlewood, Phys. Rev. B **70**, 155327 (2004).

[38] E. Whittaker and G. Watson, *A Course of Modern Analysis* (Cambridge University Press, Cambridge, UK, 1927).

[39] J. M. Kosterlitz and D. J. Thouless, J. Phys. C **6**, 1181 (1973).

[40] P. Nozières and S. Schmitt-Rink, J. Low Temp. Phys. **59**, 195 (1985).

[41] D. R. Nelson and J. M. Kosterlitz, Phys. Rev. Lett. **39**, 1201 (1977).

[42] V. N. Popov, *Functional Integrals in Quantum Field Theory and Statistical Physics* (D. Reidel, Dordrecht, 1983), Chap. 6.

[43] U. Al Khawaja, J. O. Andersen, N. P. Proukakis, and H. T. C. Stoof, Phys. Rev. A **66**, 013615 (2002).
[44] A. Griffin, *Excitations in a Bose-condensed Liquid* (Cambridge University Press, Cambridge, England, 1994).
[45] L. P. Pitaevskii and S. Stringari, *Bose-Einstein Condensation* (Clarendon Press, Oxford, 2003).
[46] P. R. Eastham, M. H. Szymanska, and P. B. Littlewood, Solid State Commun. **127**, 117 (2003).
[47] P. B. Littlewood, P. R. Eastham, J. M. J. Keeling, F. M. Marchetti, B. D. Simons, and M. H. Szymanska, J. Phys.: Condens. Matter **16**, S3597 (2004).
[48] F. M. Marchetti, M. H. Szymanska, P. R. Eastham, B. D. Simons, and P. B. Littlewood, Solid State Commun. **134**, 111 (2004).
[49] H. Haken, Rev. Mod. Phys. **47**, 67 (1975).
[50] D. M. Whittaker, Phys. Rev. B **63**, 193305 (2001).
[51] P. R. Eastham and D. M. Whittaker, Phys. Rev. B **68**, 075324 (2003).
[52] M. H. Szymanska and P. B. Littlewood, Solid State Commun. **124**, 103 (2002).
[53] M. H. Szymanska, P. B. Littlewood, and B. D. Simons, Phys. Rev. A **68**, 013818 (2003).
[54] Y. Ohashi and A. Griffin, Phys. Rev. Lett. **89**, 130402 (2002).
[55] A. Abrikosov, L. Gorkov, and I. Dzyaloshinski, *Methods of Quantum Field Theory in Statistical Physics* (Dover, New York, 1975).